

NUMERICAL ANALYSIS OF 1/28 SCALED HTGR REACTOR BUILDING TEST
FACILITY RESPONSE TO DEPRESSURIZATION EVENT

A Thesis

by

MUSTAFA ALPER YILDIZ

Submitted to the Office of Graduate and Professional Studies of
Texas A&M University
in partial fulfillment of the requirements for the degree of
MASTER OF SCIENCE

Chair of Committee,	Yassin A. Hassan
Committee Members,	Maria King
	William H. Marlow
	Rodolfo Vaghetto
Head of Department,	Yassin A. Hassan

December 2017

Major Subject: Nuclear Engineering

Copyright 2017 Mustafa Alper Yildiz

ABSTRACT

Depressurized Loss of Forced Cooling (DLOFC) accident is an important type of accident scenario in High Temperature Gas-Cooled Reactor (HTGR) design which is initiated by a break in Helium Pressure Boundary (HPB). This class of accident scenarios results in a depressurization of primary helium coolant system with subsequent release of helium into the Reactor Building (RB) and to the atmosphere through Vented Low Pressure Containment (VLPC). After the total depressurization of helium depending on the specific accident scenarios, it is also possible that air enters into the Reactor Pressure Vessel (RPV) through the RB which can potentially react with fuel and the reactor internal components such as nuclear-grade graphite.

In this study, GOTHIC model of a 1/28-scaled simplified test facility was developed to analyze the depressurization scenarios and validate them against the experimental data. Simulations were conducted in three phases by following the experiment sequence. In the first phase, natural leakage from the RB was modeled with two different methods to prepare the model for further analysis. In the second phase, post-depressurization refill of air into the RB compartments was analyzed and results were validated against experimental data. In third phase, two hypothetical depressurization scenarios were analyzed and results were compared with experimental data. Simulation results were found to be consistent with experimental data.

ACKNOWLEDGMENTS

I would like to acknowledge the support of my committee: Dr. Yassin Hassan, Dr. Maria King, Dr. William Marlow and Dr. Rodolfo Vaghetto. I would like to thank my advisor, Dr. Yassin Hassan, who provided me the opportunity and financial support to be a part of this amazing research group. I would like to thank Dr. Rodolfo Vaghetto for providing me guidance and technical knowledge during my graduate studies.

I would like to thank Zachry Nuclear for providing me the computer code used to perform the academic computational study presented in this thesis. Thanks to my lab colleagues for making my time a great experience at Texas A&M University. Special thanks to my good friend and colleague Se Ro Yang. I was privileged to have worked with him and benefit from his knowledge.

CONTRIBUTORS AND FUNDING SOURCES

Contributors

This work was supported by a thesis committee consisting of Professor Yassin A.Hassan, Professor Emeritus William H. Marlow and Research Assistant Professor Rodolfo Vaghetto of the Department of Nuclear Engineering and Professor Maria King of the Department of Mechanical Engineering.

The experimental data was provided by the Texas A&M University Department of Nuclear Engineering Thermal-Hydraulic Research Laboratory. All other work conducted for the thesis was completed by the student independently.

Funding Sources

Graduate study was supported by a fellowship from Ministry of National Education of Republic of Turkey. Part of the experimental data used for the validation have been produced within the framework of a project funded by the DOE (DE-NE-0008324).

NOMENCLATURE

BSOUP	Bounded Second Order Upwind
CFD	Computational Fluid Dynamics
DLOFC	Depressurized Loss of Forced Circulation
DOE	Department Of Energy
EPA	Energy Policy Act
FLSOUP	Flux-Limiter Second Order Upwind
FOUP	First Order Upwind
GA	General Atomics
GT-MHR	Gas Turbine-Modular Helium Reactor
HPB	Helium Pressure Boundary
HTGR	High Temperature Gas Reactor
INL	Idaho National Laboratory
LOFC	Loss of Forced Cooling
LRF	Leak Rate Factor
MFOUP	Modified First Order Upwind
MHTGR	Modular High Temperature Gas Reactor
NGNP	Next Generation Nuclear Plant
PBMR	Pebble-Bed Modular Reactor
RB	Reactor Building
RPV	Reactor Pressure Vessel

SC-HTGR	Steam Cycle High Temperature Gas-Cooled Reactor
SC-MHR	Steam-Cycle Modular Helium Reactor
SG	Steam Generator
TAMU	Texas A&M University
TC	Thermal Conductor
USNC	Ultra Safe Nuclear Corporation
VLPC	Vented Low Pressure Compartment

TABLE OF CONTENTS

	Page
ABSTRACT	ii
ACKNOWLEDGMENTS	iii
CONTRIBUTORS AND FUNDING SOURCES	iv
NOMENCLATURE	v
TABLE OF CONTENTS	vii
LIST OF FIGURES	ix
LIST OF TABLES.....	xi
1. INTRODUCTION.....	1
2. SCOPE OF THE STUDY	5
3. TEST FACILITY	6
4. GOTHIC CODE	12
5. COMPUTATIONAL MODEL.....	14
5.1 GOTHIC Model	14
5.2 Discretization of Each Control Volume	21
5.2.1 Volume 1s (CV1)	21
5.2.2 Volume 2s (CV3)	22
5.2.3 Volume 4s (CV4)	23
5.2.4 Volume 5s (CV5)	24
5.2.5 Volume 6s (CV6)	25
5.2.6 Volume 7s (V34), Volume 8s (V64(a)) and Volume 9s (V36).....	26
6. METHODOLOGY	30
6.1 Phase I - Natural Leak Rate Configuration for GOTHIC model	31
6.1.1 Determination of Leakage Flow	32
6.2 Phase II - Post-Depressurization Refill of Air into the RB Compartment	34

6.3	Phase III - Hypothetical Depressurization Scenario	36
7.	RESULTS AND DISCUSSION	39
7.1	Phase I	39
7.1.1	Initial and Boundary Conditions	39
7.1.2	Results and Discussion	41
7.2	Phase II	46
7.2.1	P2-A	47
7.2.1.1	Initial and Boundary Conditions P2A-CV1	47
7.2.1.2	Initial and Boundary Conditions for P2A-CV3&6	48
7.2.2	Results and Discussion	49
7.2.3	P2-C	54
7.2.3.1	Initial and Boundary Conditions	54
7.2.3.2	Results and Discussion	54
7.3	Phase III	56
7.3.1	P3A-1	57
7.3.1.1	Initial and Boundary Conditions	58
7.3.1.2	Results and Discussion	58
7.3.2	P3A-2	61
7.3.2.1	Initial and Boundary Conditions	62
7.3.2.2	Results and Discussion	62
8.	CONCLUSIONS	67
9.	FUTURE WORK	69
	REFERENCES	70

LIST OF FIGURES

FIGURE	Page
1.1 HTGR Prismatic Core Configuration [1]	2
3.1 Simplified RB Schematic [2]	6
3.2 CAD Drawing of TAMU NGNP Test Facility [2]	10
5.1 GOTHIC Model Nodalization Diagram.....	15
5.2 Volume 1s Nodalization	22
5.3 Volume 2s Nodalization	23
5.4 Volume 4s Nodalization	24
5.5 Volume 5s Nodalization	25
5.6 Volume 6s Nodalization	26
5.7 Volume 7s Nodalization	27
5.8 Volume 8s Nodalization	28
5.9 Volume 9s Nodalization	29
6.1 Simplified RB Design Configuration for Phase II tests [3].....	35
6.2 Expected Flow Paths for Hypothetical Depressurization Scenario Experiments [3].....	37
7.1 RPV Wall Temperature Profile	40
7.2 Comparison of Calculated (Leak Path) and Measured Pressure Decay Curves	42
7.3 Comparison of Calculated (Leakage Tool) and Measured Pressure Decay Curves	44

7.4	Phase 2 GOTHIC Model Nodalization.....	46
7.5	P2A RPV Wall Temperature Profiles.....	48
7.6	P2-A(1) Pressure Response.....	50
7.7	P2-A(1) Oxygen Concentration	51
7.8	P2-A(2) Pressure Response.....	52
7.9	P2-A(2) Oxygen Volume 6s	53
7.10	P2-C Pressure Response	55
7.11	P2-C Oxygen Concentration Inside Facility	56
7.12	Phase 3 GOTHIC Model Nodalization.....	57
7.13	P3A-1 Pressure Response.....	59
7.14	P3A-1 Oxygen Concentration	60
7.15	P3A-1 Oxygen Concentration at 420 Seconds.....	61
7.16	P3-A(2) Pressure Response.....	63
7.17	P3-A(2) Volume 2s Bottom Oxygen Concentration	64
7.18	P3-A(2) Volume 2s Bottom Oxygen Concentration	65
7.19	P3-A(2) Volume 2s Bottom Oxygen Concentration	66

LIST OF TABLES

TABLE		Page
3.1	Component Description of Simplified RB model [2].....	7
3.2	Identified Dimensionless Numbers [2].....	9
5.1	Component Description of GOTHIC Model.....	16
5.2	Support Structure Effect on Free Volume	19
5.3	Summary of Coarse GOTHIC Model Volume Subdivisions	19
5.4	Summary of Fine GOTHIC Model Volume Subdivisions.....	20
7.1	Target Leak Rate for each compartment in Texas A&M University (TAMU) test facility	39
7.2	Leak Path Hydraulic Diameters	41
7.3	Leak Rate Factors	43
7.4	Leak Rate Adjustment Based on Test Results	45

1. INTRODUCTION

Next Generation Nuclear Plant (NGNP) project was established under Energy Policy Act of 2005 which includes research, development, design, construction and operation of a prototype plant to generate electricity and to produce hydrogen. The program for the NGNP project is managed by Idaho National Laboratory (INL) [4]. The focus for commercializing the modular HTGR technology has shifted from a Department of Energy (DOE)-based NGNP project to an industry-based effort led by the NGNP Industry Alliance Limited [1]. The HTGR is one of the six alternative nuclear technologies recommended by Generation IV International Forum which is the only reactor exceptionally suited for both high-efficiency electricity production and nuclear-assisted hydrogen production [5].

In 2007, preconceptual designs of pebble-bed and prismatic based plants were developed based on prior work on the Pebble-Bed Modular Reactor (PBMR) Demonstration Pilot Plant, the General Atomics (GA) Gas Turbine-Modular Helium Reactor (GT-MHR), and Modular High Temperature Gas Reactor (MHTGR) and the AREVA Antares designs [5]. The NGNP Industry Alliance selected AREVA's 625 MWt Steam Cycle High Temperature Gas-Cooled Reactor (SC-HTGR) as the reactor design concept of choice to provide high temperature process steam for industrial applications [1]. The pebble bed reactor design concept is limited to a lower rating per module compared to prismatic design to achieve a practical reactor design that fulfills the inherent safety features at the desired operating conditions [1]. Also, for a typical total installed plant capacity in the range 2400-3000 MWt, 625 MWt prismatic block reactor modules are more cost effective compared to pebble bed reactor modules [1].

The HTGR is a graphite-moderated, helium-cooled reactor with thermal neutron spectrum that can supply nuclear heat and electricity over a range of core outlet temperatures

between 700 and 950°C, or more than 1000°C in future [6]. Core arrangement of a prismatic core configurations is shown in Figure 1.1 [1]. The inner and outer hexagonal blocks with graphite form reflector where the central hexagonal fuel blocks form the active core. HTGR core consists 10 fuel blocks height with 102 fuel columns in each block.

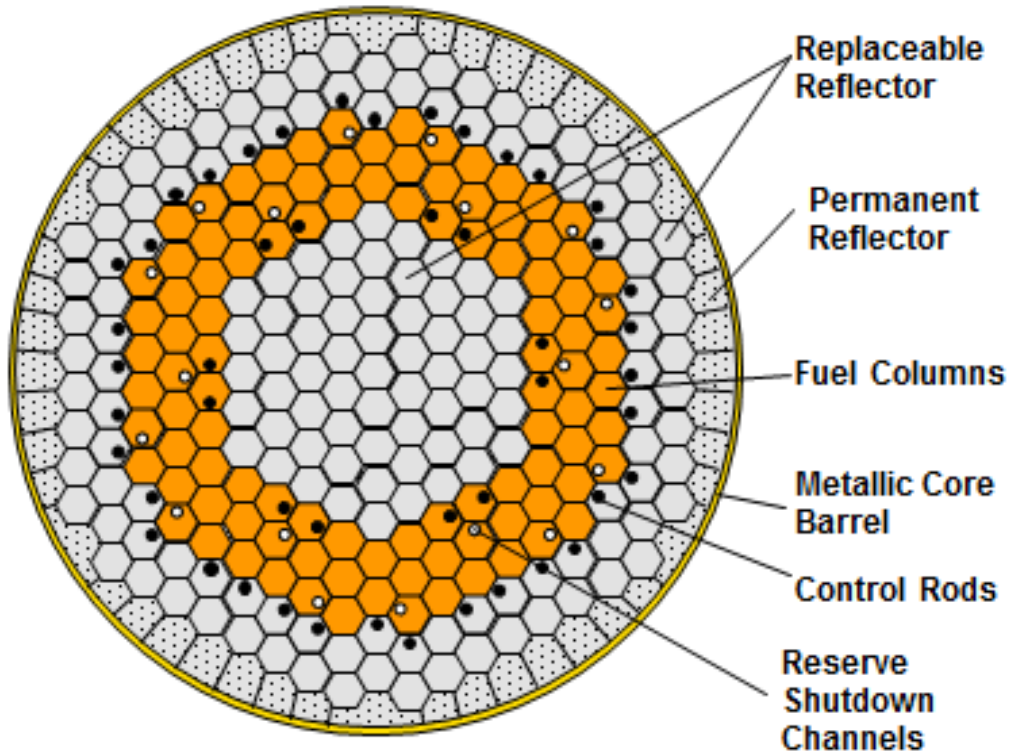


Figure 1.1: HTGR Prismatic Core Configuration [1]

HTGR technology provides improved safety and security through its inherent design. Design includes multiple layers of ceramic coating on the nuclear fuel, the carbon encasement and the graphite core structure to prevent the release of radioactive material, natural and directly to the earth heat removal without need of power or cooling fluid, chemically compatible reactor materials that in combination will not react or burn to produce heat or explosive gases [1].

Conceptual design of HTGR such as Steam-Cycle Modular Helium Reactor (SC-MHR), proposed by GA, has VLPC instead of conventional pressure-retaining low-leakage reactor containment structure as a RB design [7, 8]. During the normal operation VLPC is maintained at slightly negative pressure. In case of an accident scenario which results in VLPC internal pressures exceeding prescribed limits, the VLPC will passively vent through prescribed paths to the atmosphere [8]. These vent paths typically include one-way louvers that passively open (from differential pressure) and close (by gravity) according to the over-pressure setpoint. Use of VLPC will eliminate transport force for the fission products in the case of depressurization events such as DLOFC accident scenario [8]. After the depressurization, due to the flow reversal it is possible that VLPC design may allow air to enter through venting and leak paths into the RB compartments [8]. Depending on the specific accident scenario and primary coolant break size, ingress of air into the reactor pressure vessel may result in oxidation of fuel elements and other nuclear grade graphite, so that it may weaken the structural strength and impact the fission-product-retention capability of the fuel elements [9, 10].

Depressurization accident scenarios can be initiated over a spectrum of sizes ranging from the more likely small and moderate leaks to less likely large breaks [11]. Small break events, such as instrumentation breaks and moderate break events, involving break in a pressure relief line on top of the steam generator vessel are within the design basis of HTGRs. Large break events, involving vessel failure are beyond the design basis.

The depressurization scenarios can be split into three phases as depressurization/ blow-down phase of helium into RB, an air refill phase (from outside atmosphere into the RB), and air ingress phase (from RB atmosphere into the HPB) [2]. The blowdown phase starts with a break in HPB and ends when the depressurization ends. In air refill phase, helium leaks from the building and replaced by air. Following the air refill phase, air (oxygen) can enter through the break location and react with nuclear grade graphite structures

within the RPV.

RB response characteristics were investigated in the case of hypothetical moderate break occurring in the reactor cavity at TAMU NGNP test facility [2]. Details of the experimental facility and its specifications are given in chapter 3. Computational model which represents the experimental facility as well as with the assumptions on the model are explained in chapter 5. Results of the simulations and comparison with the experimental data is discussed in chapter 7. Finally conclusion and possible future work of this study with the limitations of the computational model are discussed in chapter 8 and chapter 9.

2. SCOPE OF THE STUDY

Objectives of this study can be categorized in four major headings:

1. Identify and select the most appropriate system (containment) code to conduct the simulations of the scenarios under consideration.
2. Create a computational model faithfully representing the geometrical characteristics of the experimental facility as well as the features which will allow to simulate experimental scenarios.
3. Validate the simulation results against experimental data.
4. Identify any limitations of the computational model and provide suggestions for future model improvements.

3. TEST FACILITY

The experimental data in this study are from tests performed during an experimental activity conducted on a dedicated test facility at TAMU NGNP test facility. The main objective of the performed tests were to obtain data on the RB pressure response and atmosphere composition suitable for code/methods validation of depressurization scenarios in support of Modular Helium Reactor (MHR) safety design and regulatory licensing objectives. Test facility is scaled, designed, and constructed based on the full scale simplified RB model [2]. Figure 3.1 represents the schematic of simplified RB design provided by Ultra Safe Nuclear Corporation (USNC).

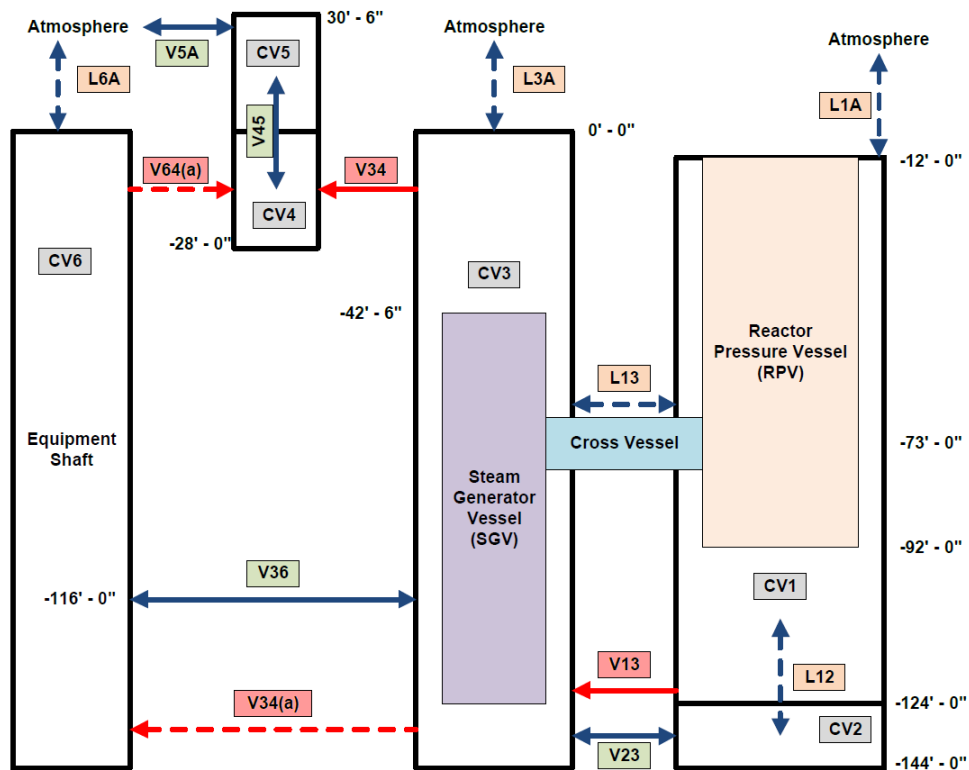


Figure 3.1: Simplified RB Schematic [2]

Description of each component of simplified RB model is provided in Table 3.1 [2].

Table 3.1: Component Description of Simplified RB [2]

Component ID	Description	Dimensions (H×W×D) [m]
CV1	Reactor Compartment	34.14×8.66×8.66
CV2	SG Dump Tank Compartment	6.10×8.66×8.66
CV3	Steam Generator Compartment	43.89×8.66×8.66
CV4	Lower Vent Space	8.53×5.76×5.76
CV5	Upper Vent Space	9.30×5.76×5.76
CV6	Equipment Shaft	43.89×5.39×5.39
RPV	Reactor Pressure Vessel	6.83×24.38 (D×L)
SGV	Steam Generator Vessel	4.51×24.38 (D×L)
V5A	RB Vent Path-Fixed Louvers	3.05×3.96×1.07
V13	One-way Vent Louver (check valve)	0.24×2.13 (D×L)
V23	Manway Door (not used in the tests)	0.91×2.44×2.13
V34	Connection between CV3 and CV4	3.05×3.96×1.07
V36	Connection between CV3 and CV6	4.27×4.27×1.07
V45	Connection between CV4 and CV5	3.05×3.96×1.07
V64(a)	Alternative vent path	3.05×3.96×1.07
L1A	Leak Path CV1-Atmosphere	-
L3A	Leak Path CV3-Atmosphere	-
L6A	Leak Path CV6-Atmosphere	-
L12	Leak Path CV1-CV2	Closed
L13	Leak Path CV1-CV3	Closed

Dimensions are in terms of height, width, and depth for square columns, and diameter and length for cylinders. L12 and L13 were not used in the test.

TAMU NGNP test facility was scaled down based on the simplified RB design by adopting dimensionless similarity-based scaling [2]. Five dimensionless numbers were identified to characterize the major thermal-hydraulic phenomena expected to occur in the RB during the air refill phase and to maintain the dynamic similarity between the full-scale simplified RB and the test facility [2]. Expected thermal hydraulic phenomena can be listed as follows

- vertical stratification and mixing
- horizontal stratification (gravity current)
- gas thermal expansion and contraction
- molecular diffusion of the binary gas mixture (air-helium).

Table 3.2 shows the five dimensionless numbers which were selected to characterize the above mentioned phenomena to maintain the dynamic similarity between the full-scale simplified RB and the scaled test facility [2]. Schmidt number was chosen to characterize diffusion between two gases [2]. Froude number is the ratio of flow inertia to external field and is chosen because the mixture is composed of two fluids (gases) [2]. It is obvious that buoyancy forces will affect the flow because of the molecular mass difference of two gases. For this reason richardson number is chosen to characterize buoyancy effects [2]. Grashof number is also related to buoyancy force effect [2]. Reynolds number was chosen to characterize the flow conditions [2].

Table 3.2: Identified Dimensionless Numbers [2]

Dimensionless Number	Formula	Description
Schmidt Number	$Sc = \frac{\nu}{D}$	Ratio of momentum diffusivity and mass diffusivity
Froude Number	$Fr = \frac{U^2}{gl \frac{\Delta\rho}{\rho}}$	Ratio of flow inertia to external field
Richardson Number	$Ri = \frac{g\beta\Delta TL}{V^2}$	Ratio of momentum diffusivity and mass diffusivity
Grashof Number	$Gr = \frac{g\beta\Delta TL^3}{\nu^2}$	Ratio of the buoyancy to viscous force acting on a fluid
Reynolds Number	$Re = \frac{UL}{\nu}$	Ratio of inertial forces to viscous forces

Figure 3.2 shows the side view of CAD drawing of the 1/28 down scaled test facility. GP-01, GP-02 and GP-03 are the gas injection ports. PT-01, PT-02 and PT-03 are the pressure transducers for the pressure measurements during the tests for CV1, CV2 and CV3 respectively [2].

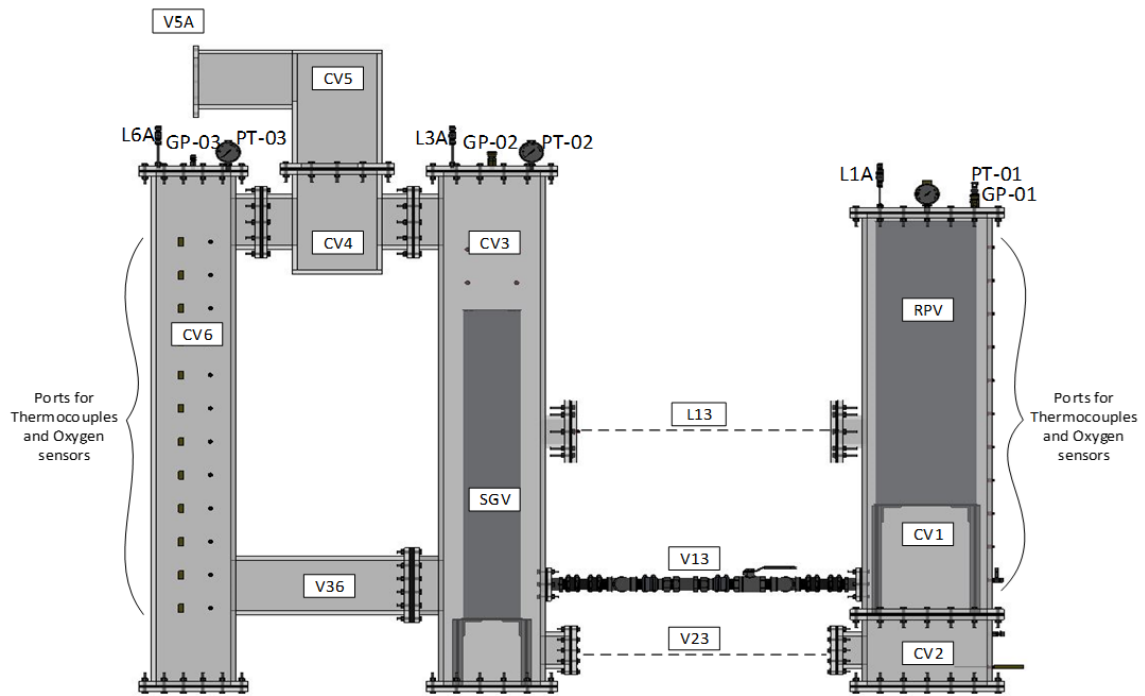


Figure 3.2: CAD Drawing of TAMU NGNP Test Facility [2]

TAMU experimental facility contains six compartments (identified with "CV") which are connected through vent paths ("V") and leak paths ("L") which connect compartments to the atmosphere. Detailed description of each component is given by Yang et al. [2].

Experiments in TAMU experimental facility were conducted to characterize the RB response during depressurization accidents. Tests were performed in three phases with each phase having the following objectives:

1. Phase I: To characterize and calibrate the test facility leak rates associated with leak paths L1A, L3A, and L6A.
2. Phase II: To characterize post-depressurization re-fill of air into the RB compart-

ments.

3. Phase III: To simulate depressurization events within the MHR design basis and characterize the displacement of air within the RB compartments by helium.

4. GOTHIC CODE

Among the system/containment codes, GOTHIC is the best suitable code for the present application because of its capabilities which give the opportunity to model test facility with sufficient three dimensional geometrical details and model the mixing of multiple fluids. GOTHIC 8.1 was used in the present study.

GOTHIC (Generation of Thermal Hydraulic Information in Containments) is a general-purpose thermal hydraulics software for design, licensing, safety, and operating analysis of nuclear containments and confinements, auxiliary buildings and related equipment [12].

GOTHIC solves conservation equations for mass, momentum and energy for three primary fields: steam/gas mixture, continuous liquid and liquid droplet fields. The phase balance equations are coupled by mechanistic models for interface mass, momentum and energy transfer. GOTHIC includes full treatment of the momentum transport terms in multi-dimensional models, with optional models for turbulent shear and turbulent mass and energy diffusion. Five models are available to model turbulence: mixing length, standard $k-\epsilon$, $k-\epsilon$ RNG, $k-\epsilon$ with a second order approximation for the Reynolds stress term or $k-\epsilon$ with a third order approximation for the Reynolds stress term.

GOTHIC noding scheme allows computational volumes to be treated as lumped (single node) or one-, two- or three-dimensional (subdivided), or any combination of these within a single model. Subdivision of a volume is based on orthogonal coordinates. Solid structures in GOTHIC are referred as thermal conductors. Thermal conductors are modeled as one-dimensional slabs which includes a general model for heat transfer between thermal conductors and the steam/gas mixture or the liquid. Thermal conductors can model heat transfer through natural and forced convection, boiling/condensation and radiation.

GOTHIC has four features to model hydraulic connections which are flow paths, net-

work models, cell interface connections in subdivided volumes and 3D connectors for subdivided volumes. Flow paths model hydraulic connections between any two computational cells. 3D connectors define the hydraulic connection across wall interfaces that are common to two separate subdivided volumes or between a subdivided volume and a lumped volume. GOTHIC includes set of models for operating equipments such as pumps, valves, doors etc.

5. COMPUTATIONAL MODEL

5.1 GOTHIC Model

Three-dimensional GOTHIC model with subdivided volumes is developed to represent the TAMU test facility and to perform simulations of selected tests. Two subdivisions were applied for discretization of the control volumes which are coarse and fine. Leakage from the control volumes were modeled with two different approaches which will be described in details further in this chapter.

The GOTHIC nodalization diagram is shown in Figure 5.1. Model consists of nine control volumes which represents the compartments of test facility and atmosphere, six flow paths connecting control volumes through computational cells, eight 3D connectors connecting subdivided volumes through common wall interfaces, two blockages inside Volume 1s and Volume 2s representing occupied free volume inside the control volumes by reactor pressure vessel and steam generator respectively, three doors and valve on leak paths, seven thermal conductors which represents the solid structures to model the heat transfer in Volume 1s.

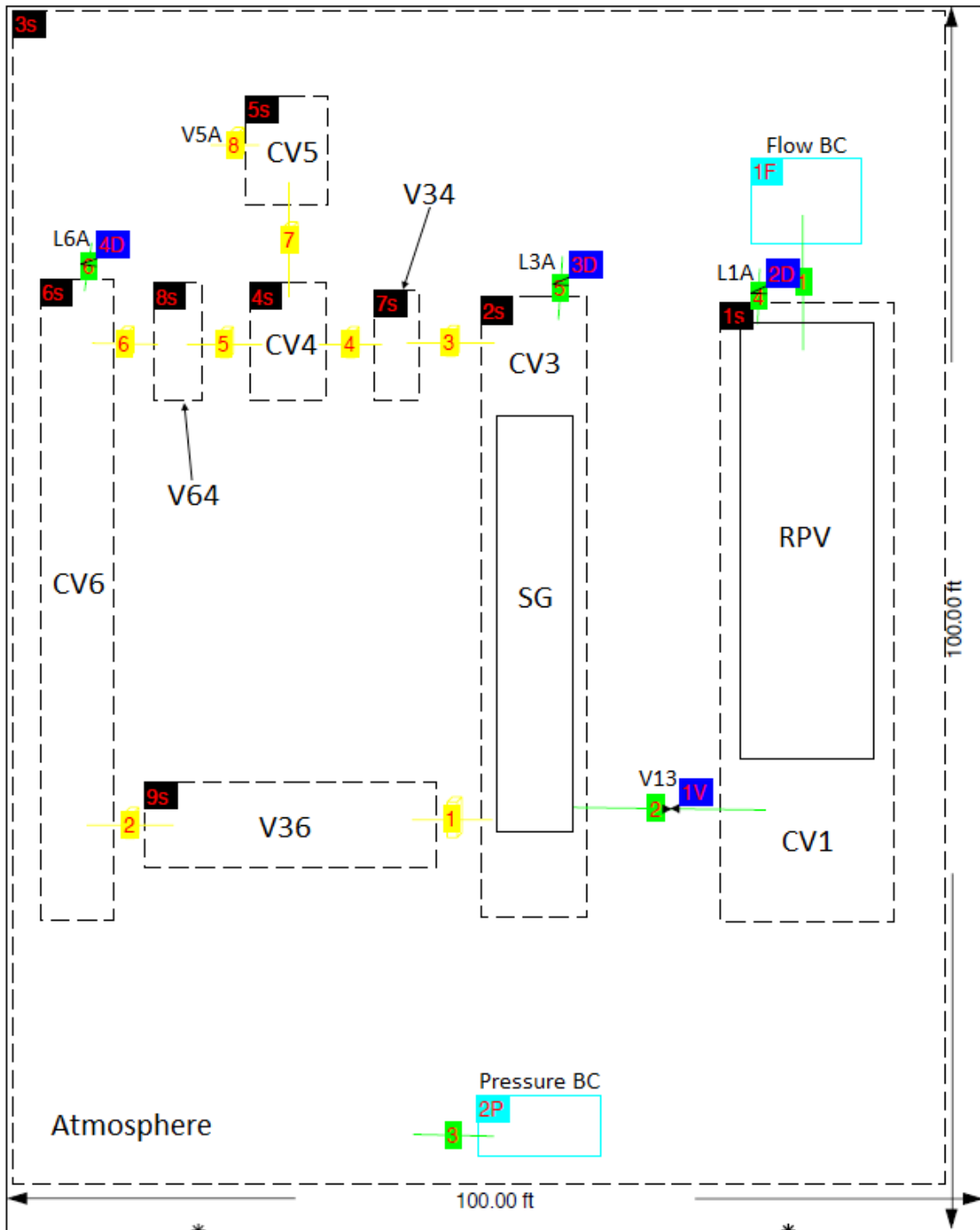


Figure 5.1: GOTHIC Model Nodalization Diagram

Description of each component of the model is given in Table 5.1.

Table 5.1: Component Description of GOTHIC Model

GOTHIC Component ID	Simplified RB Component ID	Description
Volume 1s	CV 1	Reactor Compartment
Volume 2s	CV 3	Steam Generator Compartment
Volume 3s	Atmosphere	Atmosphere
Volume 4s	CV 4	Lower Vent Space
Volume 5s	CV 5	Upper Vent Space
Volume 6s	CV 6	Equipment Shaft
Volume 7s	V34	Connection between CV3 and CV4
Volume 8s	V64(a)	Connection between CV6 and CV4
Volume 9s	V36	Connection between CV3 and CV6
FP 1	-	Connection between Reactor Compartment (CV1) and Boundary Condition
FP 2	V13	One-way Vent Louver
FP 3	-	Connection between Atmosphere (CV3) and Boundary Condition
FP 4	L1A	Leak path CV1-Atmosphere
FP 5	L3A	Leak path CV3-Atmosphere
FP 6	L6A	Leak path CV6-Atmosphere
3D Connector 1	-	Connection between CV3 and V36
3D Connector 2	-	Connection between CV3 and CV6

Table 5.1: Continued

GOTHIC Component ID	Simplified RB Component ID	Description
3D Connector 3	-	Connection between CV3 and V34
3D Connector 4	-	Connection between CV4 and V34
3D Connector 5	-	Connection between CV4 and V64(a)
3D Connector 6	-	Connection between CV6 and V64(a)
3D Connector 7	V45	Open connection between CV4 and CV5
3D Connector 8	V5A	RB vent path-Fixed louvers
Thermal Conductor (TC) 1	-	RPV Bottom Section Conductor
TC 2	-	RPV Middle Section Conductor
TC 3	-	RPV Top Section Conductor
TC 4	-	Reactor Compartment North Wall Conductor
TC 5	-	Reactor Compartment South Wall Conductor
TC 6	-	Reactor Compartment East Wall Conductor
TC 7	-	Reactor Compartment West Wall Conductor
1V	Check Valve on V13	Check Valve on One-way Vent Lower
2D	-	Door on Leak path CV1- Atmosphere
3D	-	Door on Leak path CV3-Atmosphere
4D	-	Door on Leak path CV6-Atmosphere

Since CV2 was isolated during the test activity, CV2, L12 and V23 are not included in the GOTHIC model. Cylindrical blockages were included in Volume 1s and Volume 2s to represent the space occupied by the RPV and Steam Generator (SG) respectively. For simplicity support structures for the vessels were not included in the model because they occupy relatively very small volume compared to the free volumes of CV1 and CV3. Support structure volumes were calculated by using the CAD model of the test facility and table 5.2 shows the volume of Volume 1s and Volume 2s with corresponding support structures.

Table 5.2: Support Structure Effect on Free Volume

Control Volume ID	Volume (m ³)	Support Structure Volume (m ³)	Ratio (%)
Volume 1s	7.018×10^{-2}	0.08×10^{-2}	1.14%
Volume 2s	8.078×10^{-2}	0.36×10^{-3}	0.45%

Even though CV2 is not included in the GOTHIC model, Volume 1s is modeled with reference elevation of CV2 height, to faithfully represent the actual elevations of the experimental facility.

All compartments were discretized in three dimensions. Initially discretization of the domain is made to have aspect ratio of the mesh to be as close as possible to 1. For that purpose mesh size of each side was selected to be 0.1 ft for the coarse mesh. However, 3D connectors require some special treatment to be able to connect interfaces of two volumes. On some parts of the mesh there were some modifications to match the requirements of the 3D connectors. Table 5.3 shows the coarse GOTHIC model discretization details with total number of cells in each volume.

Table 5.3: Summary of Coarse GOTHIC Model Volume Subdivisions

Volume ID	X-Direction Divisions	Y-Direction Divisions	Z-direction Divisions	Total # of Cells
Volume 1s (CV1)	11	12	20	2640
Volume 2s (CV3)	8	10	39	3120
Volume 6s (CV6)	6	8	39	1872

The discretization of the GOTHIC Model were analyzed further with a mesh sensitivity study to validate it before further simulations. Analysis were performed by simulating Phase I tests (described in Chapter 6) with finer mesh with both leakage methods, which are described in chapter 6. Volume 1s, Volume 2s and Volume 6s were subdivided finer by the factor of 2 in each direction. Table 5.4 summarizes the number of meshes in each direction and total number of cells for each volume.

Table 5.4: Summary of Fine GOTHIC Model Volume Subdivisions

Volume ID	X-Direction Divisions	Y-Direction Divisions	Z-direction Divisions	Total # of Cells
Volume 1s (CV1)	22	24	40	21120
Volume 2s (CV3)	16	20	78	24960
Volume 6s (CV6)	12	16	78	14976

For the mesh sensitivity analysis, pressure was chosen to be the quantity of interest because of two reasons. Firstly, in this study main focus was on depressurization of the volumes and the gas concentration inside the volumes during or after the depressurization. GOTHIC uses ideal gas law to find the gas concentrations inside the control volume. Second reason why pressure played a big role in this study is because depressurization curves were used to find the leak rates from the compartments, as it is described in chapter 6.

The results of the sensitivity study using GOTHIC leakage tool showed that mass leak rates at one psid for volumes 2s and 6s for coarse and fine meshes were the same and the relative error for volume 1s between two discretizations is 1.65%. The leak path method showed a similar result for volumes 2s and 6s, whose mass leak rates for coarse and fine meshes were the same; further, for volume 1s, the relative error was less than 2%. As the

error was in acceptable range, further cases were simulated with a coarse mesh to reduce the computational time.

5.2 Discretization of Each Control Volume

5.2.1 Volume 1s (CV1)

Volume 1s¹ (CV1) represents the reactor compartment. Part of the volume is occupied by a cylindrical region to represent the RPV. This is modeled using the "blockage" feature available in GOTHIC software. The model of the reactor vessel is divided into three sections of equal height and three thermal conductors have been included to it (one in each section). Thermal conductors corresponding to RPV walls have 0.05112 inch thickness. Temperatures, measured in experiment with thermocouples, are applied as boundary conditions to the left side (inner side of blockage) of each thermal conductor. RPV wall conductor surface option is set to "Correlation set". Natural convection option is set to Rayleigh-number-dependent correlation ($h = (k/l)CRa^n$) [12]. Outer side of CV1 compartment walls were assumed to be at constant atmospheric temperature. For this reason, there is a thermal conductor assigned to each compartment wall. Thermal conductors of compartment walls have thickness of 0.5 inches which represents the compartment wall thickness. Conductor surface option for Volume 1s compartment wall is set to correlation set and natural convection option is set to vertical surface with default GOTHIC minimum convection heat transfer coefficient. Figure 5.2 shows the Volume 1s (CV1) nodalization. In the same figure, thermal conductors 4s, 5s, 6s and 7s represents the north, south, east and west compartment walls respectively.

¹Subdivided Component

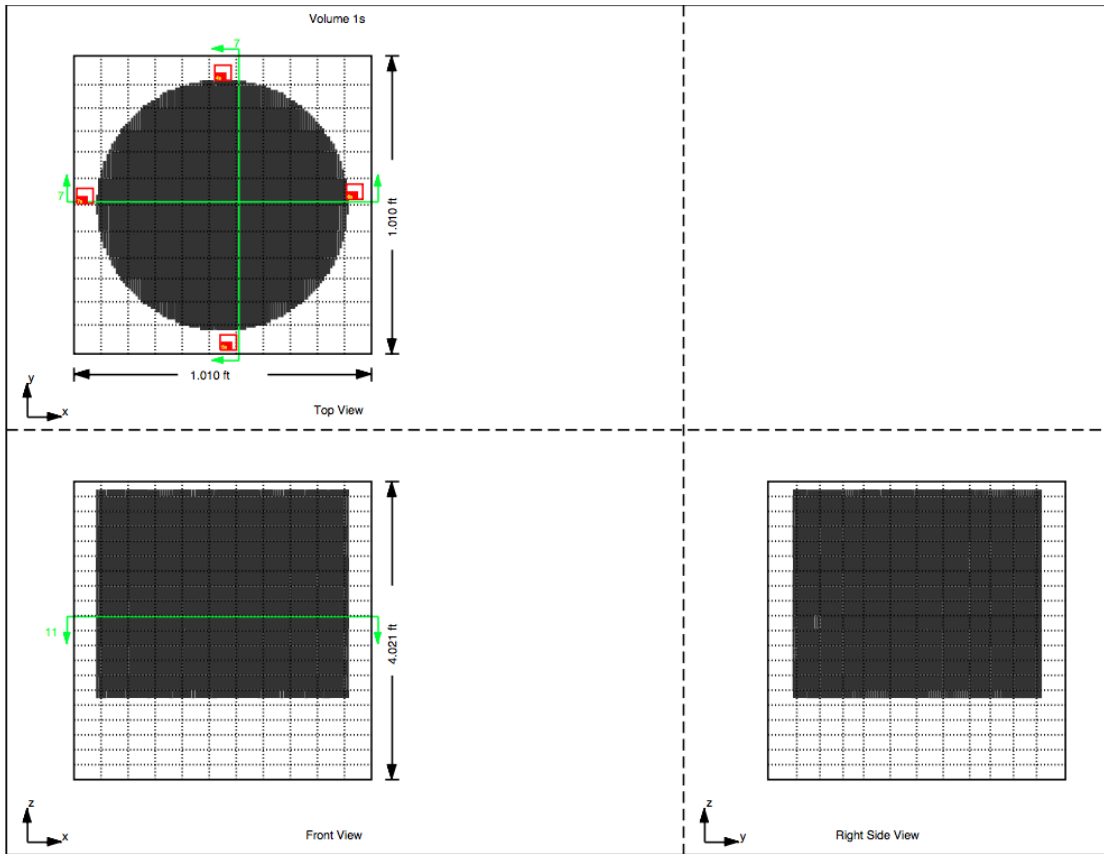


Figure 5.2: Volume 1s Nodalization

5.2.2 Volume 2s (CV3)

Volume 2s (CV3) represents the steam generator compartment. CV3 has a cylindrical blockage which represents the SG. SG is modeled as a single cylindrical blockage. Steam generator walls were not producing heat in the experiments. Since isothermal conditions have been used during the experiments on CV3, no thermal conductors have been defined for this compartment. Three dimensional subdivisions in the upper and lower sections of this volume have been optimized (refined) in the y and z-directions to match the 3D connectors used as flow paths with adjacent compartments. Figure 5.3 represents the nodalization for Volume 2s.

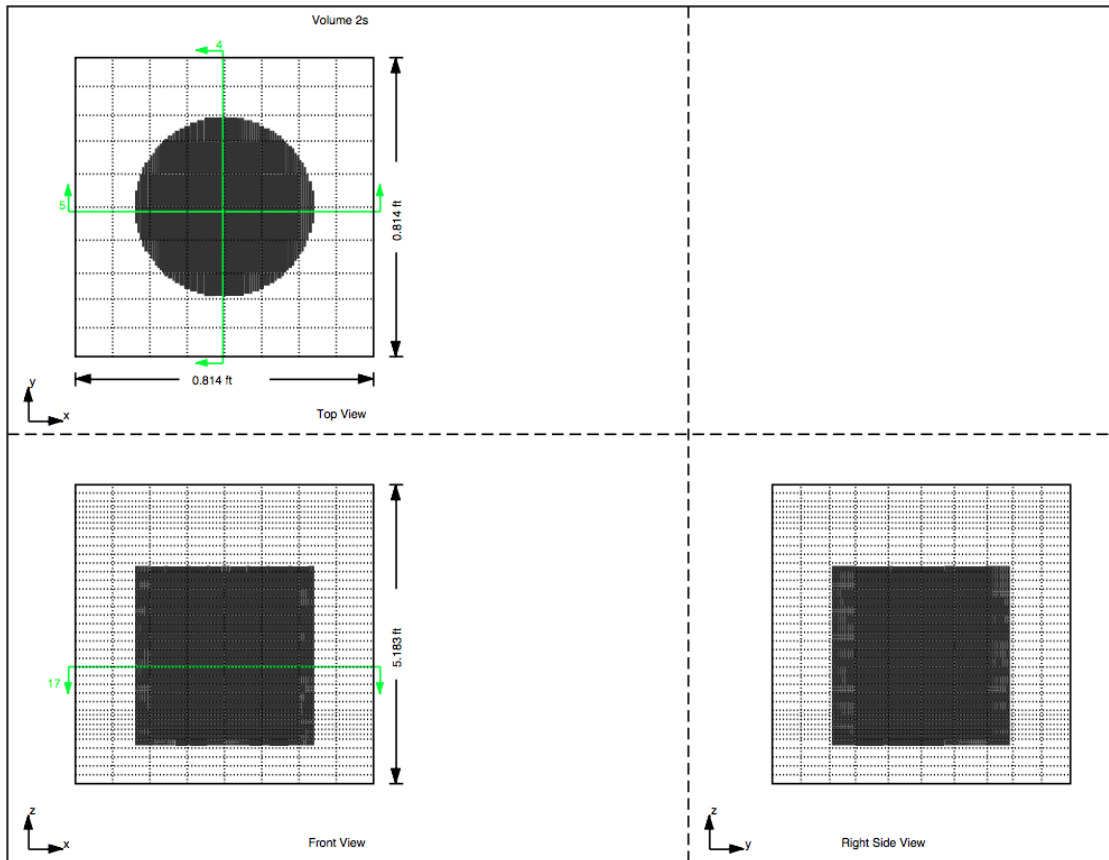


Figure 5.3: Volume 2s Nodalization

5.2.3 Volume 4s (CV4)

Volume 4s (CV4) represents the Lower Vent Space. It is modeled as a subdivided volume with no blockage to represent the free volume of the experimental facility. Nodalization of Volume 4s can be seen in Figure 5.4.

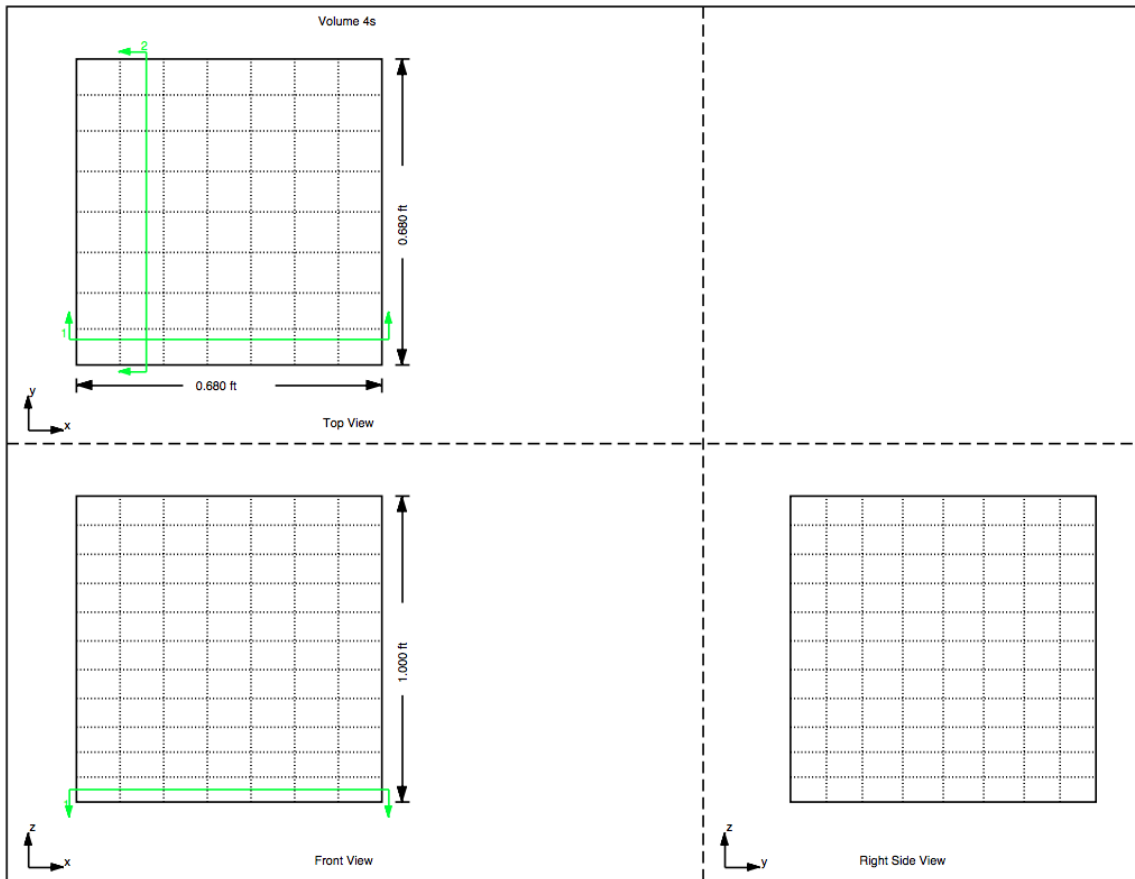


Figure 5.4: Volume 4s Nodalization

5.2.4 Volume 5s (CV5)

Volume 5s (CV5) represent the Upper Vent Space. It is modeled as a subdivided volume with no blockage to represent the free volume of the experimental facility. Nodalization for Volume 5s can be seen in Figure 5.5.

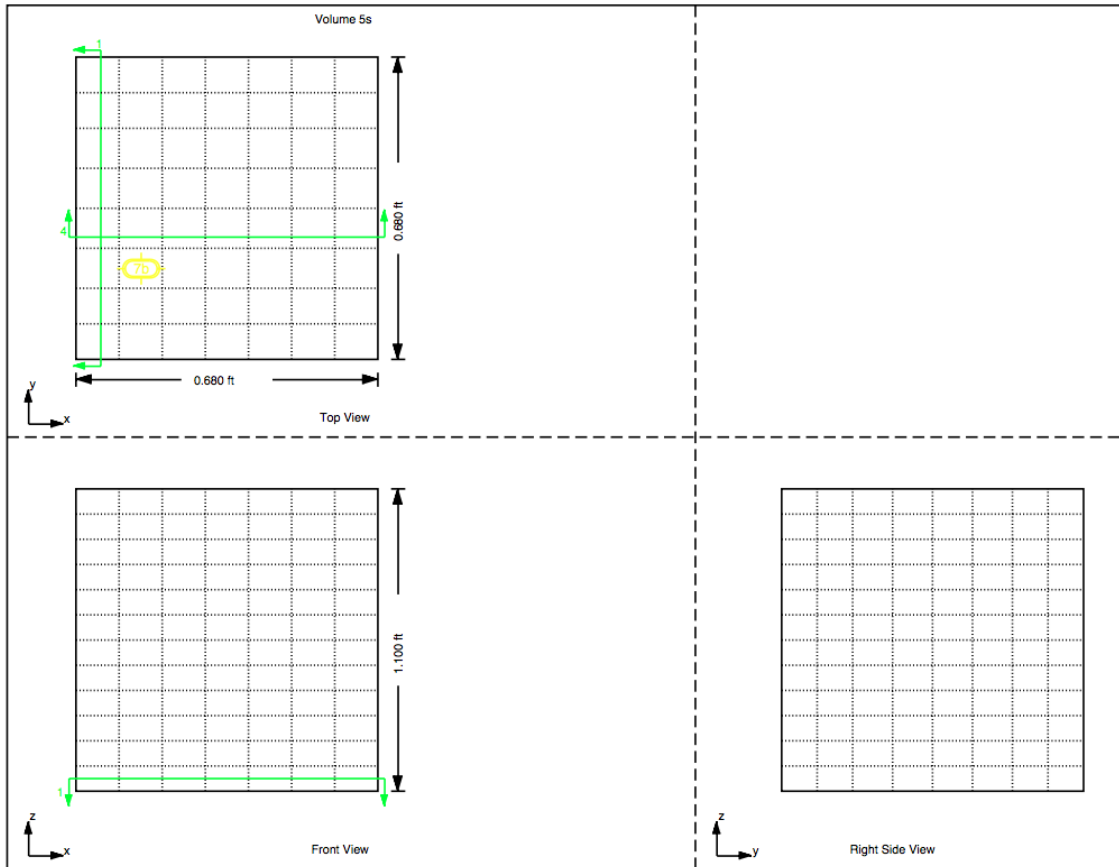


Figure 5.5: Volume 5s Nodalization

5.2.5 Volume 6s (CV6)

Volume 6s (CV6) represents the equipment shaft. This is modeled as a subdivided volume with no blockage to represent the free volume of the experimental facility. This subdivided component has a finer mesh size in the z-direction in the upper and lower regions and optimized in y-direction, to meet the meshing approach used to connect Volume 2s with Volume 8s and Volume 9s. Figure 5.6 represents the nodalization for Volume 6s.

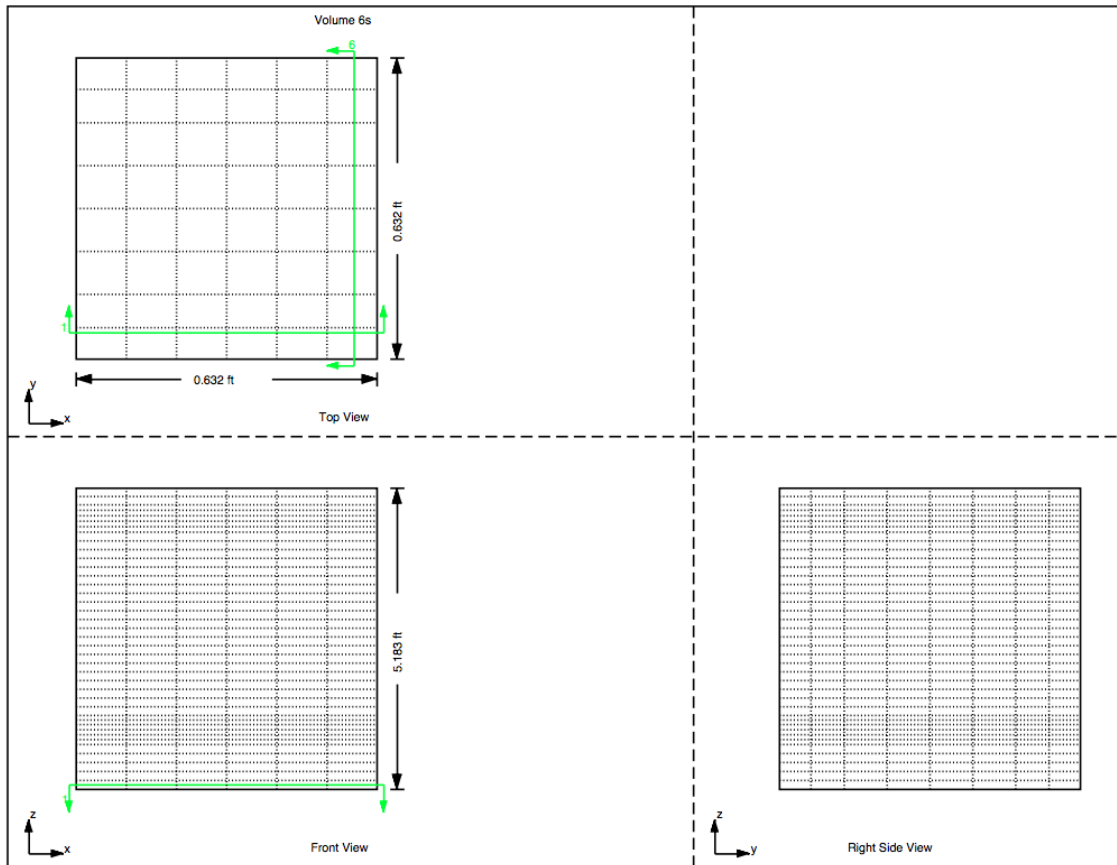


Figure 5.6: Volume 6s Nodalization

5.2.6 Volume 7s (V34), Volume 8s (V64(a)) and Volume 9s (V36)

Due to their size in the experimental facility, some of the venting paths have been modeled using subdivided control volumes instead of flow paths. These were also connected with the main compartments using 3D connectors.

Volume 7s (V34) represents the connection between Volume 2s and Volume 4s. Nodalization of Volume 7s can be seen in Figure 5.7. Volume 8s (V64a) represents the connection between Volume 6s and Volume 4s. Volume 9s (V36) represents the connection between Volume 2s and Volume 6s. Nodalization for Volume 8s and Volume 9s can be seen in Figure 5.8 and Figure 5.9 respectively.

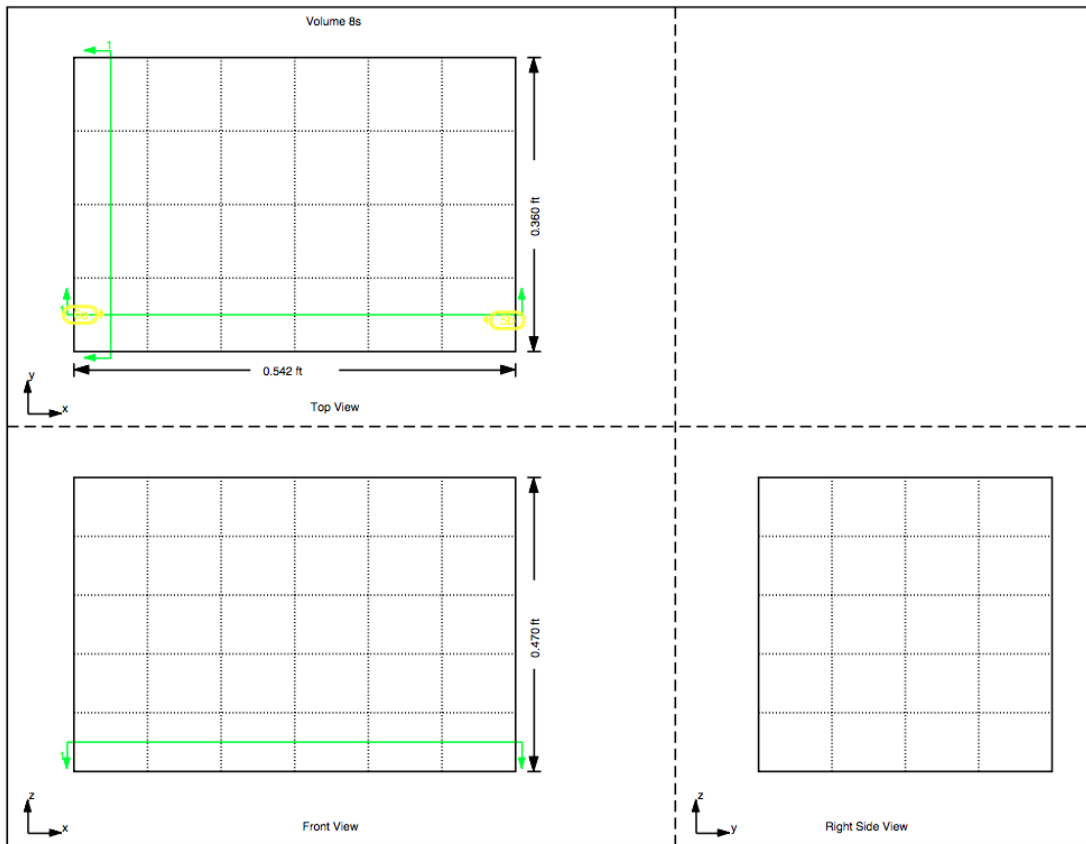


Figure 5.7: Volume 7s Nodalization

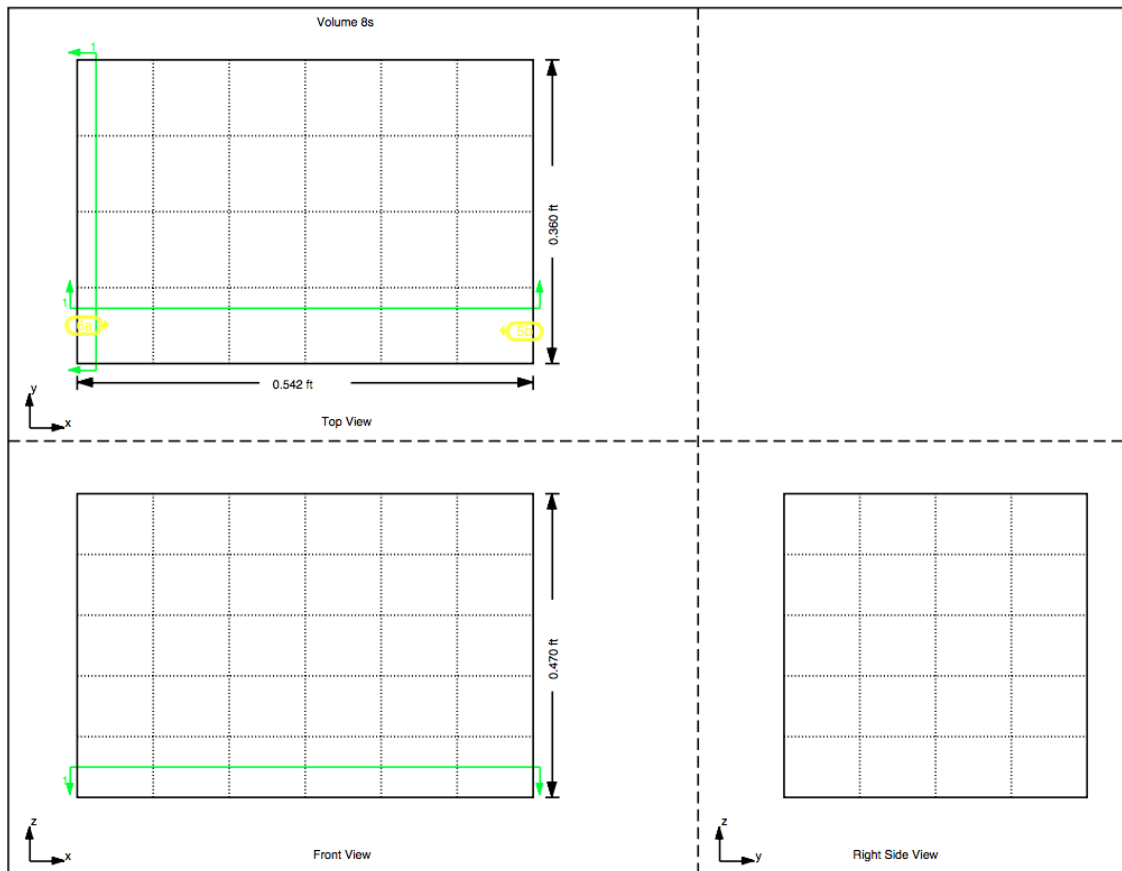


Figure 5.8: Volume 8s Nodalization

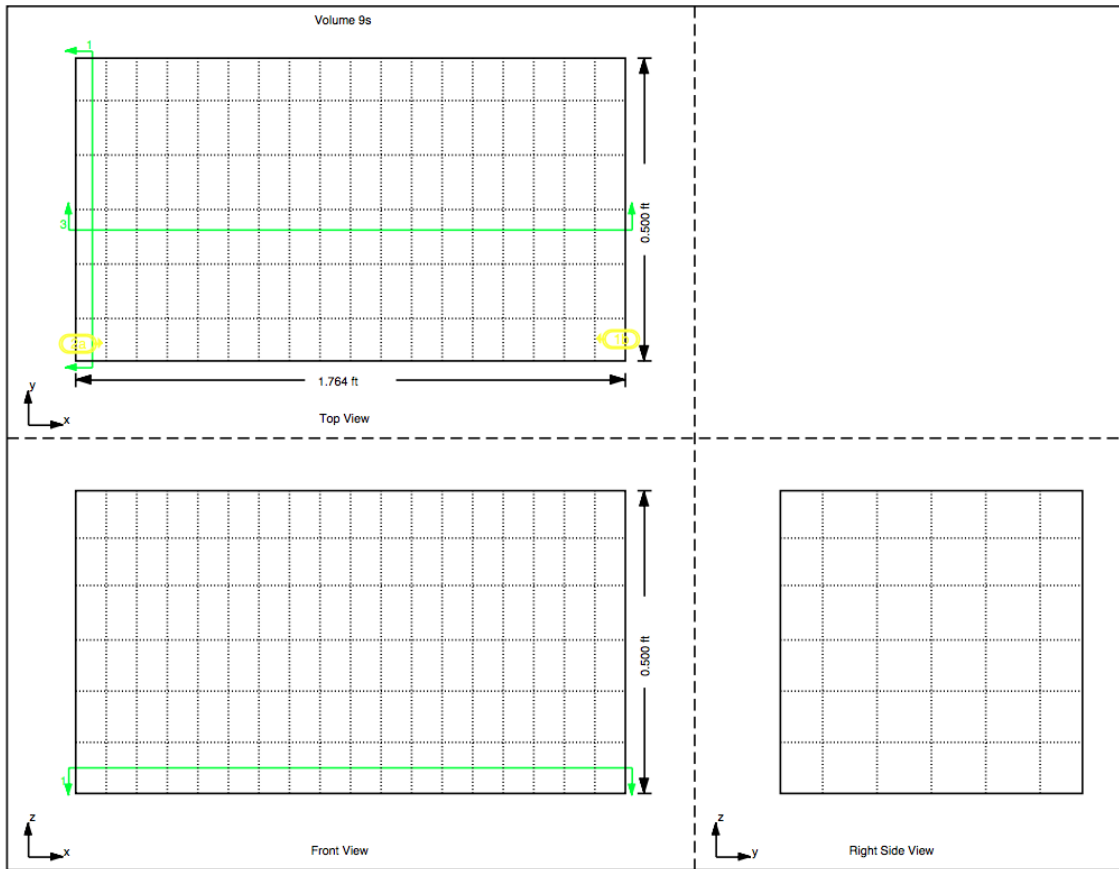


Figure 5.9: Volume 9s Nodalization

6. METHODOLOGY

Experiments are simulated with GOTHIC in three phases by adopting the test sequence. First phase is simulated to adjust the leak rates from control volumes 1s, 2s and 6s to the target values obtained from the experimental results. In second phase, simulations are performed to characterize the post depressurization refill of air into the compartments. Final phase consists the simulation of hypothetical accident scenario. GOTHIC model incorporates some practical assumptions/simplifications as discussed below:

1. Support structures for the RPV and SG are not modeled because of their relatively small dimensions (impact on compartment free volume is approximately 1% or less).
2. CV2 and V23 are not included in the model, which is consistent with the experimental test matrix. The height of CV2 is accounted to represent the actual elevations of the test facility.
3. The cross vessel is not included in the model, since large-scale breaks were not part of the experimental test matrix and beyond the design capabilities of the test facility.
4. For simplicity one-way vent path louver V13 is modeled as a quick open/close valve.
5. Three heat conductors were used to simulate the RPV walls at the top, middle, and bottom sections (corresponding to thermocouple locations). The measured temperatures were imposed as boundary conditions, assuming the temperatures are uniform within each of the three sections.
6. The oxygen concentration in 100% air is assume to be 21% by volume.

6.1 Phase I - Natural Leak Rate Configuration for GOTHIC model

Current NGNP HTGR RB conceptual design specifies the RB natural leak rate as the total RB volume per day through the leak path, with a 1 psig constant pressure for the full-scale plant. Contributions of the major compartments to the natural leak rate is 20% (CV1-Volume 1s), 30% (CV3 - Volume 2s) and 50% (CV6 - Volume 6s). The purpose of the Phase I - Natural leak rate configuration simulations are to tweak parameters in the model to reach the target experimental leak rates for the facility and prepare the model for the further accident scenario analysis.

Two different methodologies are adopted for adjusting leak rates from volumes 1s, 2s and 6s. Figure 3, Figure 4 and Figure 5 shows the discretization of each mentioned control volume.

First method simulates leak rates by use of leak paths L1A, L3A and L6A on top of volumes 1s, 2s and 6s respectively. Pressure drop through a leak path can be expressed as:

$$\Delta P = \frac{fl}{D_h} \frac{\rho v^2}{2} \quad (6.1)$$

where ΔP is pressure difference, f is friction factor calculated by GOTHIC solver, l is friction length, ρ is fluid density, D_h is hydraulic diameter and v is fluid velocity [12]. To match the mass flow rate to the target value (experimental value), adjustments can be made to two of the free parameters of Equation 6.1, such as friction length, and the hydraulic diameter, as pressure difference, density, and friction factor (calculated by code) are fixed. To simplify the process, the friction length is fixed to average thickness of the compartment walls. Adjustments are made to the hydraulic diameter, D_h , to match the leak rates for each compartment to the target experimental results.

During the leak rate test for CV1 (Volume 1s), cylinder inside the CV1 compartment was heated. To simulate the same conditions, time dependent temperature recordings in-

side the RPV wall are applied as boundary conditions to the thermal conductors associated with the RPV in GOTHIC model. Heat transfer through Volume 1s compartment walls is modeled by imposing constant room temperature on the outer side of thermal conductors associated with compartment walls. A Rayleigh number dependent natural convection option is used for the interface with the Volume 1s compartment atmosphere.

Second method to model the leak rate from the compartments is by the use of leakage model provided by GOTHIC code. There are two options provided by the code, laminar and turbulent leakage models, which are applicable to lumped and subdivided volumes and available to predict the flow through small and not so small cracks, respectively [12]. Based on the given definition, laminar leakage model is adopted for our case. Leak paths L1A, L3A and L6A are removed from the facility model and leakage option is applied to volumes 1s, 2s and 6s. Leakage option requires specific factor to be defined for the volume such as Leakage Rate Factor (LRF) which is defined as the leaking mass percentage per hour from the volume and has units of (%/hour) and based on the total mass in the leaking volume [12].

$$\dot{m} = \frac{L_r}{100} V \rho_{v_r} \quad (6.2)$$

where L_r is the specified leak rate, V is the volume of the leaking computational volume and ρ_{v_r} is the vapor density at the reference conditions [12].LRF for each volume calculated using the experimental data for pressure decay in compartments corresponding to volumes 1s, 2s and 6s.

6.1.1 Determination of Leakage Flow

The pressure inside of the test facility is assumed decay exponentially as shown in Eq.6.3 [13]

$$\frac{dP(t)}{dt} = e^{-\lambda t} \quad (6.3)$$

where λ is the decay constant depending on the test specifications and with units of $[\text{s}^{-1}]$ and t is time. In this case pressure loss from the facility can be represented as

$$P(t) = P_0(1 - e^{-\lambda t}) \quad (6.4)$$

where P_0 is the initial pressure inside the compartment and $P(t)$ is the pressure at time t inside the compartment. Assuming the gas inside the compartment is ideal gas,

$$PV = NRT \quad (6.5)$$

Volume of the gas is constant in facility and assuming the constant gas temperature inside the facility Equation 6.5 can be rewritten as

$$P(t) = CN(t) \quad (6.6)$$

where $C = \frac{RT}{V}$ and can be assumed as constant for constant temperature. Mass leaking out from the volume is related to molar change of the gas inside the volume. It can be stated as

$$N(t) = \frac{P(t)}{C} \quad (6.7)$$

Number of moles in volume $N(t)$ can be replaced by $\frac{m(t)}{M_A}$ where $m(t)$ is mass of the gas and M_A is the molar mass of the gas.

$$m(t) = \frac{M_A P(t)}{C} \quad (6.8)$$

If we substitute Equation 6.4 into 6.8 and taking the derivative with respect to time we get,

$$\frac{dm(t)}{dt} = \frac{M_A P_0}{C} \frac{d(1 - e^{-\lambda t})}{dt} \quad (6.9)$$

It follows that leakage mass flow can be determined using the following equation:

$$\frac{dm(t)}{dt} = \frac{M P_0}{C} \lambda e^{-\lambda t} \quad (6.10)$$

where,

M - Molecular weight of the gas. Approximated as 28.9 g/mol for air.

$C = \frac{RT}{V}$

R - Universal Gas Constant which is $8.3144598 \text{ m}^3 \times \text{Pa} \times \text{K}^{-1} \times \text{mol}^{-1}$

T - Gas temperature

V - Gas volume

P_0 - Initial Pressure

The axial mean temperature was used to find the constant C .

6.2 Phase II - Post-Depressurization Refill of Air into the RB Compartment

Phase II simulations investigate the transient behaviour of air refilling into RB filled with helium at slightly higher (~ 1 psig) than atmospheric pressure. Figure 6.1 shows the test facility configuration for the post-depressurization air refill tests. Two possible RB states were investigated following the depressurization event:

1. RB vent paths operate as designed and following the depressurization only flow paths for air to displace the helium are L1A, L3A and L6A.
2. RB vent paths fail open and much larger leak paths are available for air to displace helium following the depressurization.

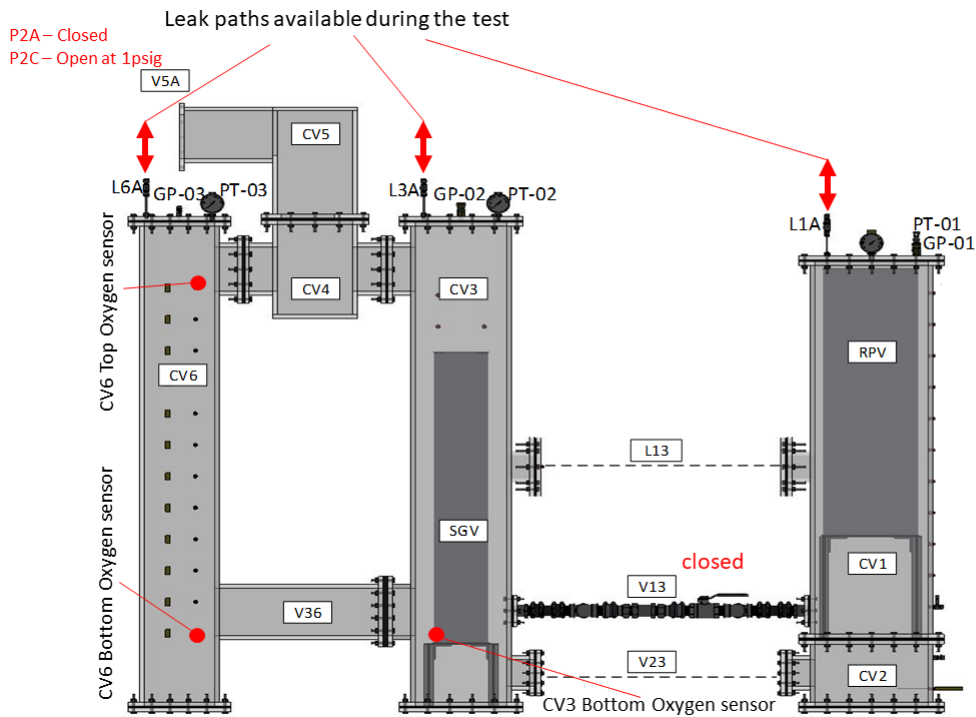


Figure 6.1: Simplified RB Design Configuration for Phase II tests [3]

Post-depressurization analysis simulations have two configurations corresponding to two possible RB states following the depressurization, P2-A and P2-C. Facility model which is used in phase II simulations consists three main volumes (1s, 2s and 6s) and volumes which connect them (volume 4s, 5s, 7s, 8s and 9s). In both configurations, cavity volumes were pressurized to 1.2 psig with 100% helium and valve 1V was closed which isolates Volume 1s from the rest of the facility [14]. For simplicity, P2-A simulations for volume 1s was called as P2-A(1) and simulations for the rest of the facility was called as P2-A(2).

P2-A(1) simulations consists only volume 1s and it was simulated separately from the rest of the facility model. RPV inside the volume 1s is heated by applying experimental temperature recordings from the RPV inner side as a boundary condition to the left side

of thermal conductors associated with blockages which represent the RPV in the model. Temperature of the outer side of the volume 1s is assumed to be at the room temperature since there is no data available from the conducted experiments. A Rayleigh number dependent natural convection option is used for the interface with the volume 1s atmosphere.

Configuration for P2-A(2) simulation consists all volumes presented in GOTHIC model except for volume 1s. RB vent path (V5A), the outlet of volume 5s to atmosphere is closed in this configuration. Only connection between cavities and atmosphere are leak paths/leakage model from volumes 2s and 6s. P2-A(2) configuration is an isothermal case at room temperature.

P2-C configuration originally consists all volumes of GOTHIC model presented in Figure 5.1, however it was simulated only for volumes included in P2-A(2) configuration, since in P2-C, volume 1s is isolated from the rest of the facility and there are no differences in initial and boundary conditions for volume 1s from P2-A(1) conditions. Initially all volumes in P2-C configuration except for Volume 3s (Atmosphere) are pressurized to 1.2 psig. V5A is closed until the pressure decays to 1 psig through leak paths/leakage model. After the pressure reaches 1 psig, trip is set to fully open V5A. P2-C configuration is isothermal at room temperature.

Simulations for post depressurization analysis were performed with both leakage methods adopted in Phase I by keeping leak paths (L1A, L3A and L6A) and applying leak path parameters in first case, and in second case by applying leakage model parameters instead of leak paths.

6.3 Phase III - Hypothetical Depressurization Scenario

Phase III simulations analyze the RB vent path configuration to depressurization scenarios. As shown in Figure 6.2, the simplified RB model includes a reference (Hinged louver position 1) and alternative (Hinged louver position 2) vent path configuration. Sim-

ulation P3A-1 simulates a hypothetical moderate-sized break at the top of the SG with reference vent path, and P3A-2 simulates a hypothetical moderate-sized break at the top of the SG with alternative vent path.

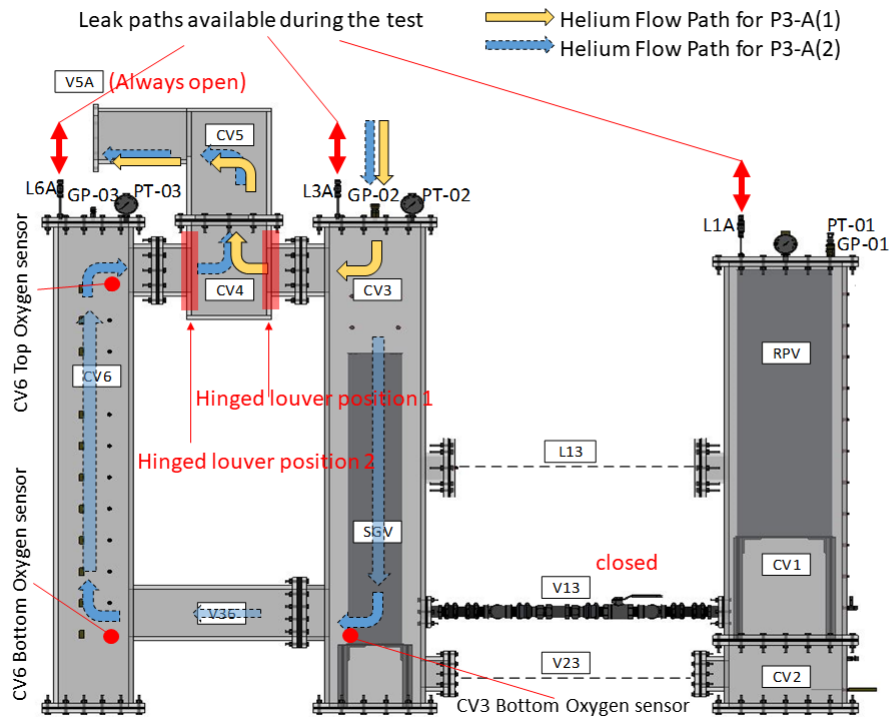


Figure 6.2: Expected Flow Paths for Hypothetical Depressurization Scenario Experiments [3]

Facility model used in phase III simulations consists all volumes except for volume 1s since in experiments CV1 is isolated from the rest of the facility with closed valve V13. Volume 2s is connected to 6s through 4s, 5s, 7s, 8s and 9s. Hinged louvers in the test facility are adopted to the GOTHIC model by adding doors to 3D connectors 4 and 5. Leak paths L3A and L6A were open in both scenarios.

Initial and boundary conditions for Phase III are obtained from the performed tests. All volumes are initially filled with 100% air at atmospheric pressure and doors at 3D

connectors 4 and 5 are closed. In both cases for Phase III simulations helium was injected from top of the volume 2s with the rate of 1.68 kg/h. Hinged louver configuration for P3A-1 is simulated by closing the door on 3D connector 5 for the entire simulation and opening the door on 3D connector 4 with trip at 1 psig. For the P3A-2, door on 3D connector 4 was closed for the entire simulation and door on 3D connector 5 was opened with trip at 1 psig. In both hinged louver configurations volume 5s was connected to atmosphere with 3D Connector 8 to represent the open V5A. Both simulations of hypothetical depressurization scenario was isothermal at room temperature.

Simulations for phase III, are performed with both leakage methods.

7. RESULTS AND DISCUSSION

Simulations are performed for all three phases described in Methodology section. In this section, simulation results are compared with experimental data.

7.1 Phase I

Phase I simulations were conducted to find appropriate parameters for leak paths L1A, L3A and L6A to tune the leak rates to the predetermined target values. In the model, L1A, L3A and L6A are simulated as a single flow paths connecting CV1, CV3 and CV6 to the atmosphere. Initial and boundary conditions for the simulations are set according to conducted experiments. Target and experimental leak rates for the main three compartments of the facility are listed in Table 7.1.

Table 7.1: Target Leak Rate for each compartment in TAMU test facility

Compartment	Volume (m^3)	Target Leak Rate (g/s)	Experiment Leak Rate [3] (g/s)
CV1	6.938×10^{-2}	3.103×10^{-3}	2.908×10^{-3}
CV3	8.042×10^{-2}	4.655×10^{-3}	4.521×10^{-3}
CV6	5.72×10^{-2}	7.759×10^{-3}	7.742×10^{-3}

7.1.1 Initial and Boundary Conditions

Target and simulation leak rate for each control volume is listed in Table 7.1. Since the purpose of this study is to represent the features and behavior of test facility, experimental leak rates were used as reference to match.

Simulation is initiated with room temperature ($22^\circ\text{C} \approx 71.6^\circ\text{F}$) for all three control volumes. Inner wall temperature of RPV cylinder is set to temperature profile given in

Figure 7.1 recorded during the experiment. Initial compartment wall temperature and atmosphere temperature are set to room temperature.

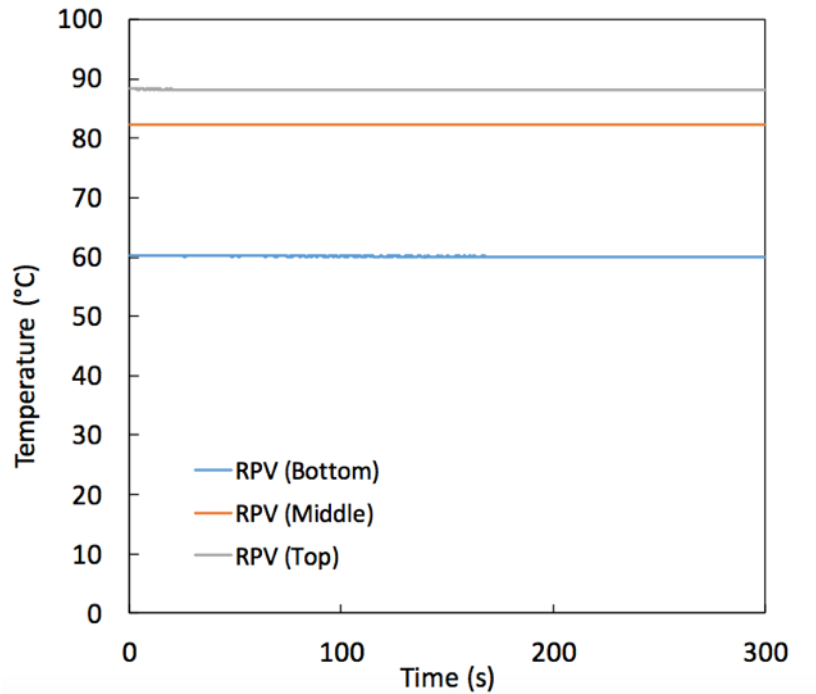


Figure 7.1: RPV Wall Temperature Profile

Initial condition for air inside of the compartment is 71.6 °F. Since pressure of gas increases with increasing temperature in a closed domain, simulation of CV1 is initiated at lower pressure (0.56 psig) to reach desired initial pressure with the effect of heating the air. Initial pressure of 0.56 psig obtained by trial and error with several preliminary short (20 seconds) simulations.

Leak rates for CV3 and CV6 simulated in isothermal (ambient temperature) conditions. Simulations for CV3 and CV6 are initiated by applying an initial pressure of 1.2 psig.

Phase 1 was simulated for 300 seconds. Solution method was set to SEMI-IMPLICIT, pressure solution method is CONJUGATE and differencing scheme is BSOUP.

7.1.2 Results and Discussion

Simulations to adjust the natural leak rates from the volumes 1s, 2s and 6s were performed with both methods described in Methodology section 6.1. Table 7.2 shows the GOTHIC model leak path hydraulic diameters that were derived as a result of sensitivity analysis to match the experimental/target leak rates.

Table 7.2: Leak Path Hydraulic Diameters

L1A (mm)	L3A (mm)	L6A (mm)
0.298	0.290	0.3427

Figure 7.2 shows the comparison of simulated (with leak paths) and measured pressure decays in Volumes 1s, 2s, and 6s with corresponding exponential fit functions. The calculations for Volume 1s include a pressurization phase to reach 1.2 psig, whereas the calculations for Volume 2s and 6s assume the initial pressure is 1.2 psig. It can be seen that GOTHIC was able to accurately simulate the measured pressure decay curves with use of single leak path to simulate the leakage from the entire volume.

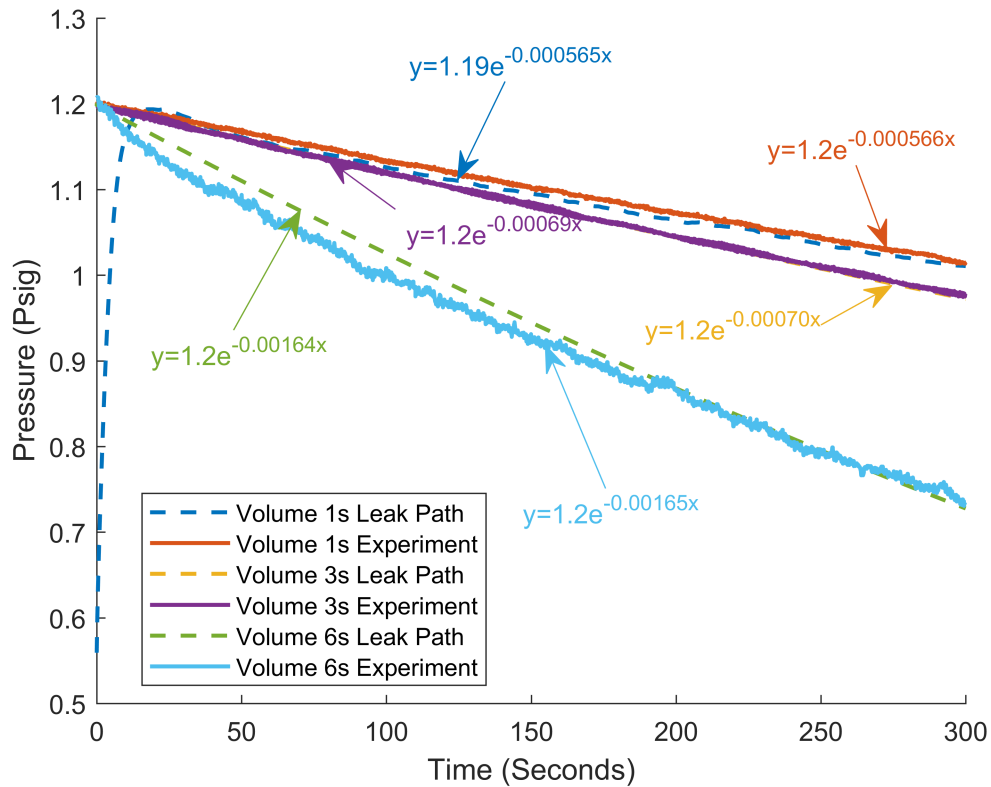


Figure 7.2: Comparison of Calculated (Leak Path) and Measured Pressure Decay Curves

Pressure decay simulations of each volume with calculated LRFs resulted in lower pressure decay rate than the target. To match the target pressure decay, sensitivity analysis were performed to LRFs for each volume. Calculated LRF from experimental data and satisfactory LRF from sensitivity analysis for each volume are presented in Table 7.3.

Table 7.3: Leak Rate Factors

	Volume 1s (%/hour)	Volume 3s (%/hour)	Volume 6s (%/hour)
Calculated LRF	6.53	6.92	7.53
Satisfactory LRF	15.66	13.4	32.2

Comparison of calculated (Leakage Tool) and measured pressure decay curves for volumes 1s, 2s and 6s are depicted in Figure 7.3. It should be noted that in both approaches calculations for volume 1s include a pressurization phase of about 20 seconds to reach 1.2 psig, whereas calculations for volumes 2s and 6s assume the initial pressure is 1.2 psig.

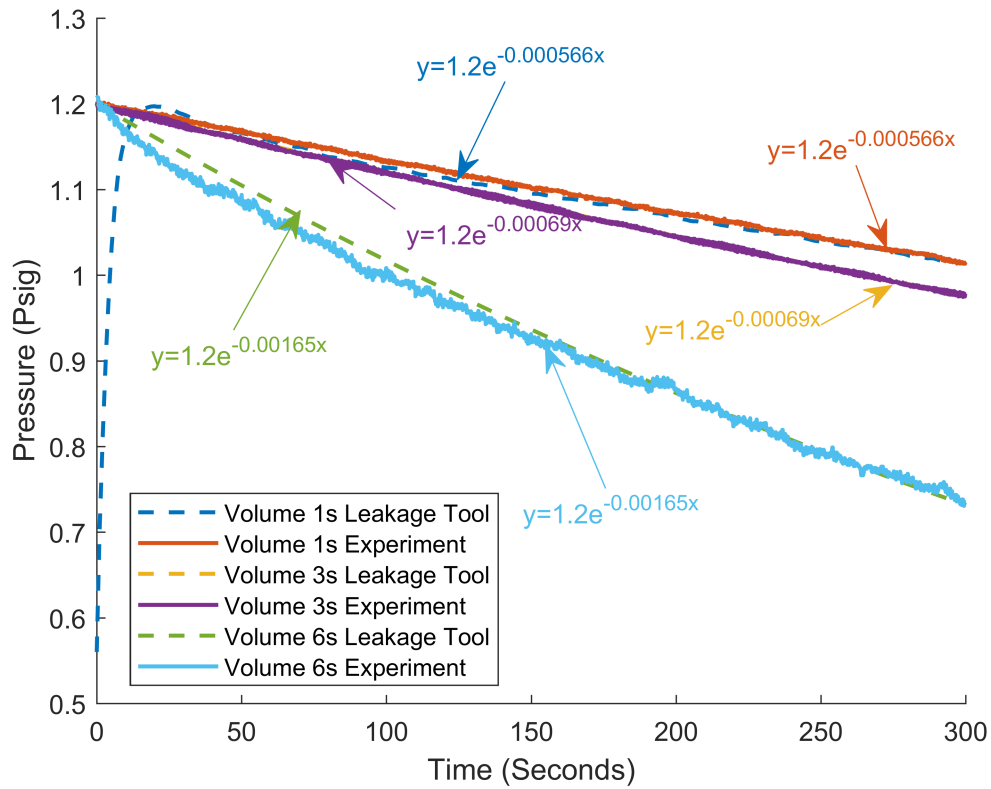


Figure 7.3: Comparison of Calculated (Leakage Tool) and Measured Pressure Decay Curves

Table 7.4 shows the adjusted leak rates simulated with both methods. Leak rates were calculated with Eq. 6.10 under a positive pressure condition of 1 psig inside the volumes 1s, 2s and 6s for the NGNP HTGR RB GOTHIC model.

Table 7.4: Leak Rate Adjustment Based on Test Results

Volume ID	Temperature (K)	Leak Rate (g/s) GOTHIC Leak Path	Leak Rate (g/s) GOTHIC Leakage Tool	Leak Rate (g/s) Experiment [3]	Relative Error (%) Leak Path	Relative Error (%) Leakage Tool
Volume 1s	322	2.917×10^{-3}	2.922×10^{-3}	2.908×10^{-3}	0.31	0.50
Volume 2s	295	4.573×10^{-3}	4.508×10^{-3}	4.521×10^{-3}	1.15	0.29
Volume 6s	295	7.621×10^{-3}	7.667×10^{-3}	7.742×10^{-3}	1.56	0.97

7.2 Phase II

Purpose of phase 2 simulations is to characterize the post-depressurization air refill phase of TAMU NGNP Test Facility. The model used for Phase 2 simulations is shown in Figure 7.4. Flow path V13 is closed during simulations to reproduce the conditions used during the experiments. Since CV1 is isolated in Phase 2 simulations, Volume 1s was simulated separately. Volume 2s and Volume 6s are connected to each other through the Volume 4s and Volume 9s. Volume 5s representing the containment chimney, is connected to atmosphere through path V5A. This flow path is maintained open or closed based on the specifications of the experimental test. Leak path parameters estimated in Section 7.1 used during this phase.

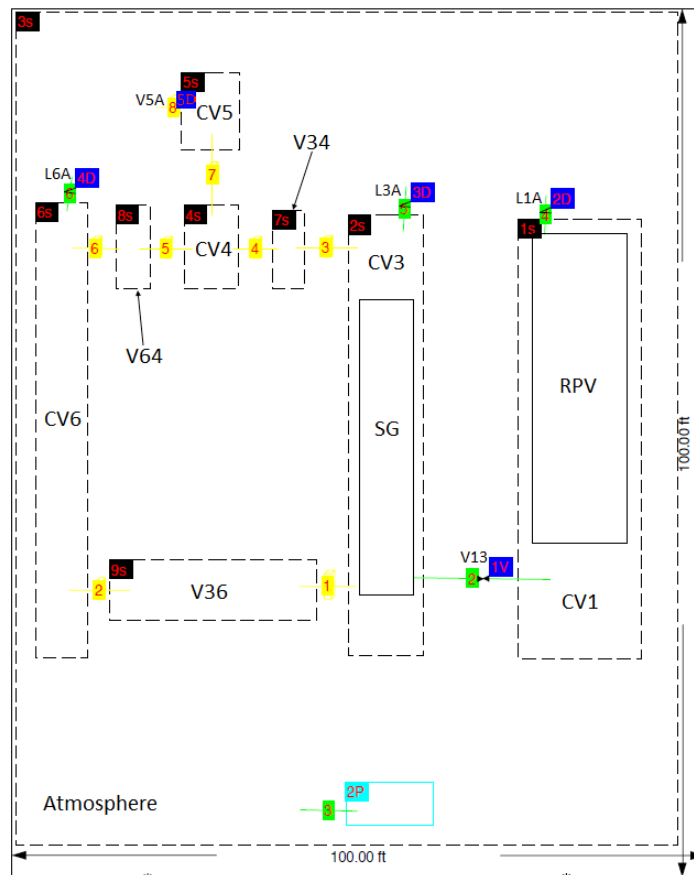


Figure 7.4: Phase 2 GOTHIC Model Nodalization

7.2.1 P2-A

P2-A simulations were performed to simulate pressure response during the post- depressurization refill of air into the control volumes. Connection between Volume 5s and atmosphere (V5A) is closed during the P2-A calculations. Initial conditions and boundary conditions used in simulations were obtained from experiments. Leak paths L1A, L3A and L6A are the only paths connecting the control volumes to the atmosphere. Volume 1s was isolated from Volume 3s and Volume 6s in simulations, consistently with the experimental setup. Since CV1 was isolated during the experiments, simulations for P2A were made separately for Volume 1s (CV1). For simplicity, simulations for CV1 are called P2A-CV1 and simulations for the CV3 and CV6 are called P2A-CV3&6.

7.2.1.1 Initial and Boundary Conditions P2A-CV1

Volume 1s is filled with 100% helium gas initially. The initial pressure of CV1 in experiment was 1.2 psig. Since Volume 1s has thermal conductors inside of it which increases the temperature and consequently the pressure of gas inside Volume 1s, initial pressure was setup to a lower value to account for pressure increase due to the heat generated in the reactor vessel. Inner wall temperatures of cylindrical blockage are set to given profiles in Figure 7.5.

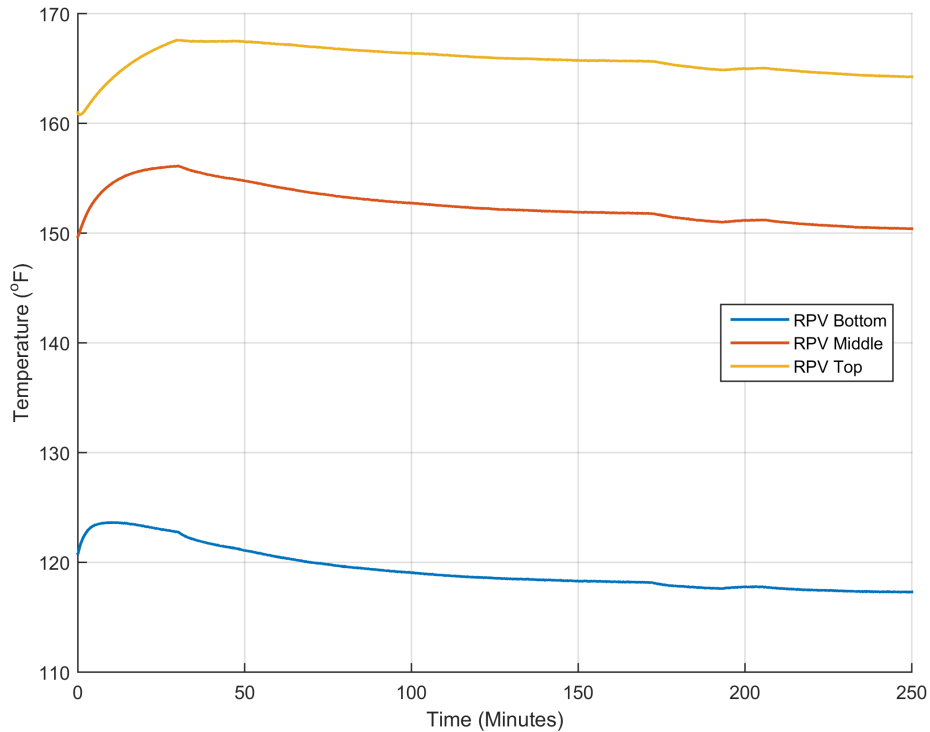


Figure 7.5: P2A RPV Wall Temperature Profiles

Initial temperature of compartment inner wall and boundary condition for atmosphere temperature are set to room temperature of 71.6 °F. Initial temperature of gas inside Volume 1s is at room temperature as well. Pressure of CV1 increased from initial pressure of 0.66 psig to 1.2 psig and decayed exponentially.

According to the experimental test duration P2A - CV1 was simulated for 15000 seconds (250 minutes). Solution method was set to SEMI-IMPLICIT, pressure solution method is CONJUGATE and differencing scheme is BSOUP.

7.2.1.2 Initial and Boundary Conditions for P2A-CV3&6

Volume 2s (CV3) and Volume 6s (CV6) are connected through Volume 4s and Volume 9s and simulated together. All compartments are filled with 100% helium gas. Initial

pressure inside the cavities are 1.2 psig. Temperature of the gas inside of the cavities is at room temperature. Volume 2s and Volume 6s simulations are isothermal.

According to the experimental test duration P2A-CV3&6 was simulated for 60000 seconds (1000 minutes). Solution method was set to SEMI-IMPLICIT, pressure solution method is CONJUGATE and differencing scheme is BSOUUP.

7.2.2 Results and Discussion

Figure 7.6 shows the comparison of pressure response for volumes 1s using both leakage models adopted in phase I with experimental data. Since the FP 2 (flow path which connects Volume 1s to volume 2s) is closed during the P2-A(1) simulation, depending on the leakage model helium leaks to atmosphere only through leak path 1 or through the walls of volume 1s with leakage tool. Leak path model underpredicts the pressure inside the volumes where leakage tool model overpredicts it.

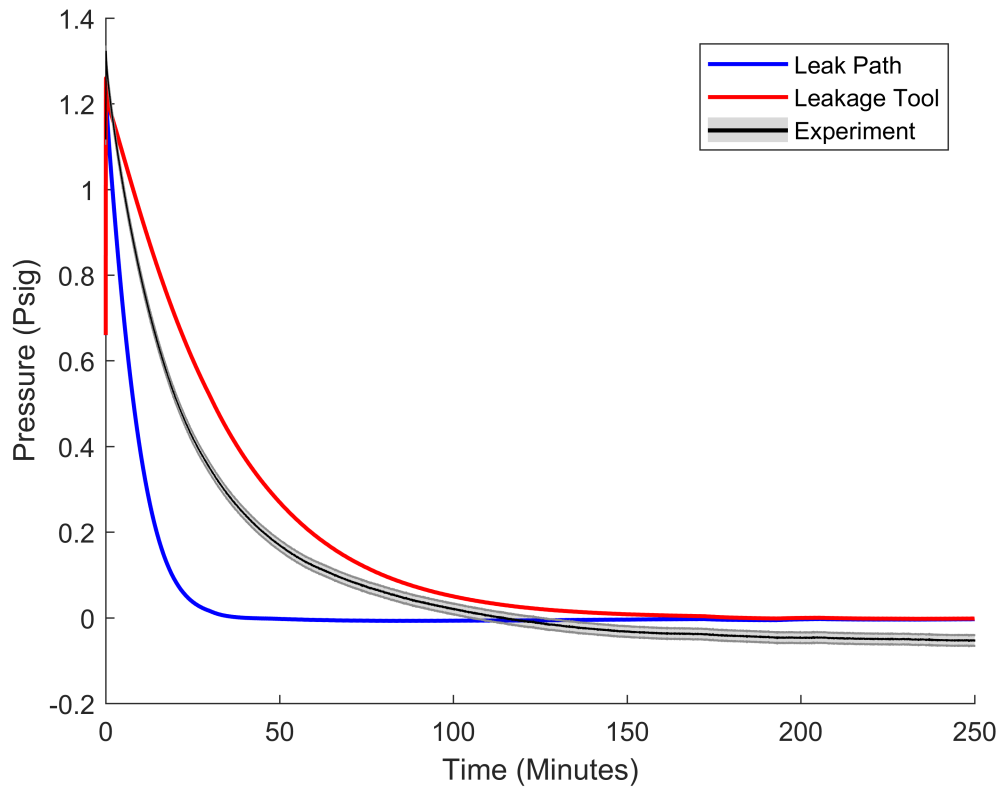


Figure 7.6: P2-A(1) Pressure Response

In experiments, oxygen concentration in volume 1s was measured at elevation near FP 2. Figure 7.7 illustrates comparison of oxygen concentration inside the volume 1s. Experimental data indicates oxygen buildup inside the volume where GOTHIC simulations show no significant rise in oxygen concentration. L1A is the only connection of volume 1s to atmosphere. After the pressure in volume 1s balances with atmospheric pressure, air fills into volume with diffusion mechanism through L1A. Leak path model in GOTHIC simulations shows increasing trend of oxygen concentration inside the volume 1s after 50 minutes of depressurization event.

GOTHIC leakage model in Figure 7.6 shows the pressure inside volume 1s balances

with atmospheric pressure at around 200 minutes after depressurization event. Which shows that oxygen concentration starts to increase inside the volume 1s around that time.

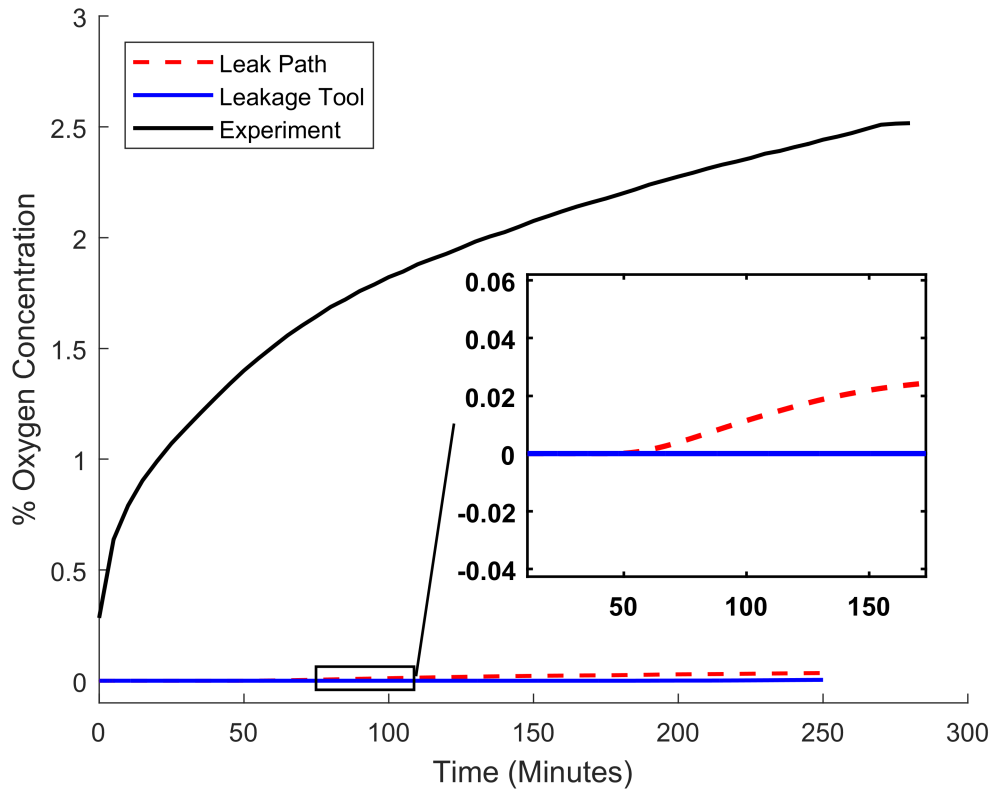


Figure 7.7: P2-A(1) Oxygen Concentration

Figure 7.8 illustrates the pressure response in volumes 2s and 6s with both leakage models. V5A was closed in P2-A(2) simulations so in case where leakage modeled with leak paths L3A and L6A were the only connections between facility and atmosphere, and walls of volume 2s and 6s for the leakage tool case. Leakage tool provided by the code has a good agreement with experimental results where for the leak path case pressure inside facility decayed to atmospheric pressure in 22 minutes which is around 5 times faster than

experimental result.

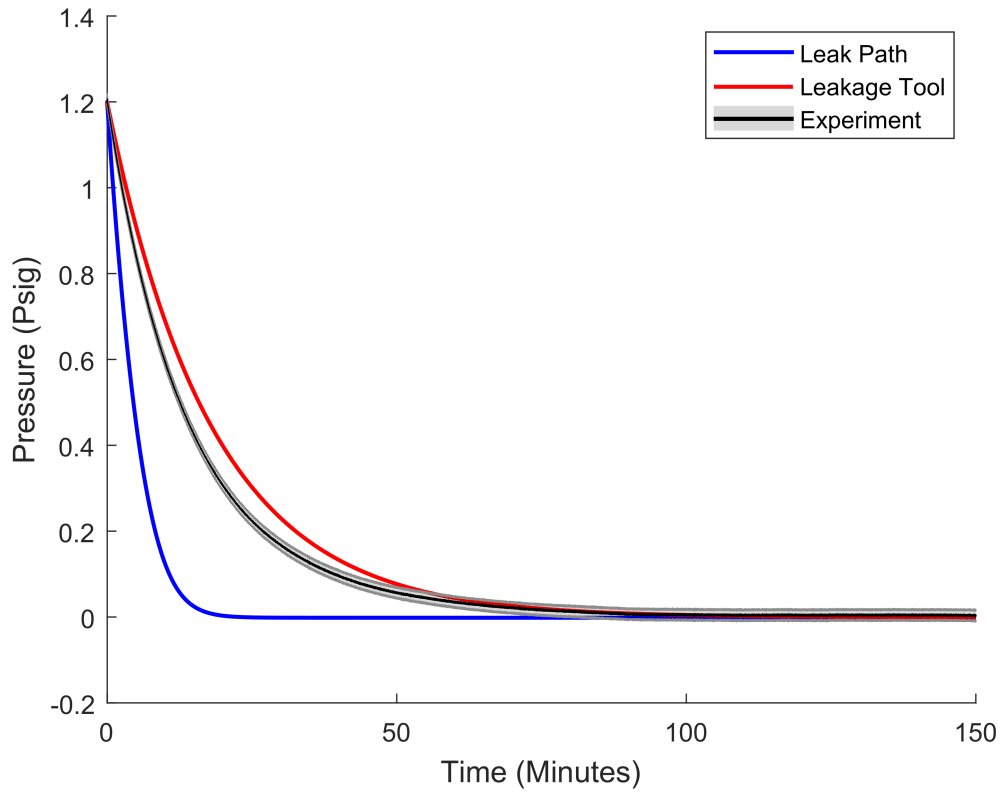


Figure 7.8: P2-A(2) Pressure Response

Figure 7.9 shows the oxygen concentration in volume 6s. Experimental results may reflect incomplete flushing of air from the test facility prior to the experiment. However, after the pressure inside the facility decayed to atmospheric pressure there is an increasing trend of oxygen concentration inside the facility.

GOTHIC simulations show essentially no air refill through the leak paths into the RB over the 1000 minutes simulation time. Leakage tool was able to capture increase in

oxygen concentration after the pressure inside the volume.

GOTHIC simulations and the experimental results show the RB design effectively mitigates air refill into the RB for long time periods following a depressurization event. Thus, the results indicate that when the vent paths close as designed RB will be isolated from the outside atmosphere for long time periods.

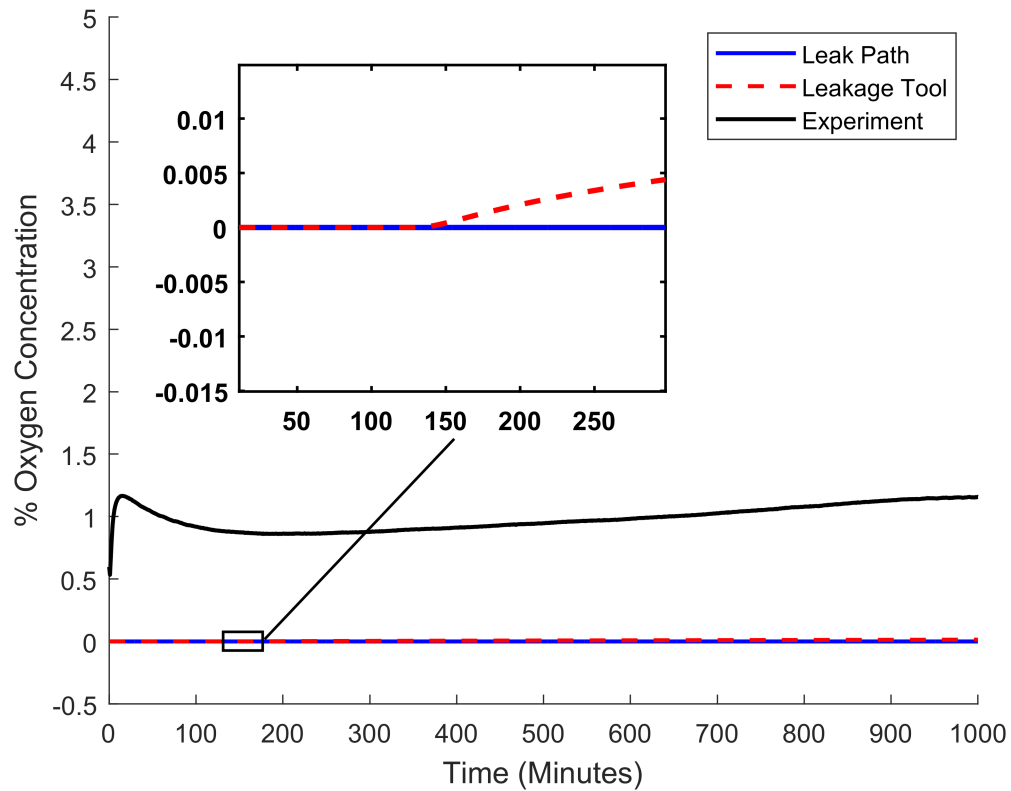


Figure 7.9: P2-A(2) Oxygen Volume 6s

7.2.3 P2-C

P2-C simulations were performed to simulate the air-refill characteristics after the depressurization event with vent path failed open. In this case, air refill occurs through the chimney (Volume 5s) as well as through the leak paths L1A, L3A and L6A. Since V13 is closed as in P2-A, CV1 is isolated from CV3 and CV6.

7.2.3.1 *Initial and Boundary Conditions*

Volume 2s and Volume 6s are connected through Volume 4s and Volume 9s. All compartments initially are filled with 100% helium gas. Initial pressure inside the cavities are 1.2 psig. Helium inside the cavities is at room temperature. Ambient air temperature is also at room temperature and pressure of ambient air is 1 atm (14.7 psia = 0 psig). Simulations performed in P2-C are isothermal.

Main difference of P2-C simulations from the P2-A is that V5A (Volume 5s) opens when the pressure decays to 1 psig through the leak paths L3A and L6A. For simplicity, horizontal part which is connected to CV5 (shown in Figure 7.4) was not included to the simulation model but the connection of Volume 5s to Volume 3s occurs through the same cross sectional area as in experimental facility.

P2C simulations were performed for 3000 seconds (50 minutes). Solution method was set to SEMI-IMPLICIT, pressure solution method is CONJUGATE and differencing scheme is BSOUP.

7.2.3.2 *Results and Discussion*

For this case, the RB vent path (V5A) is assumed to fail open when the pressure drops to 1 psig. Figure 7.10 shows the pressure response in RB compartments. As it was expected, GOTHIC simulations and experimental data show the RB compartments rapidly depressurize to ambient conditions after the vent path fails open.

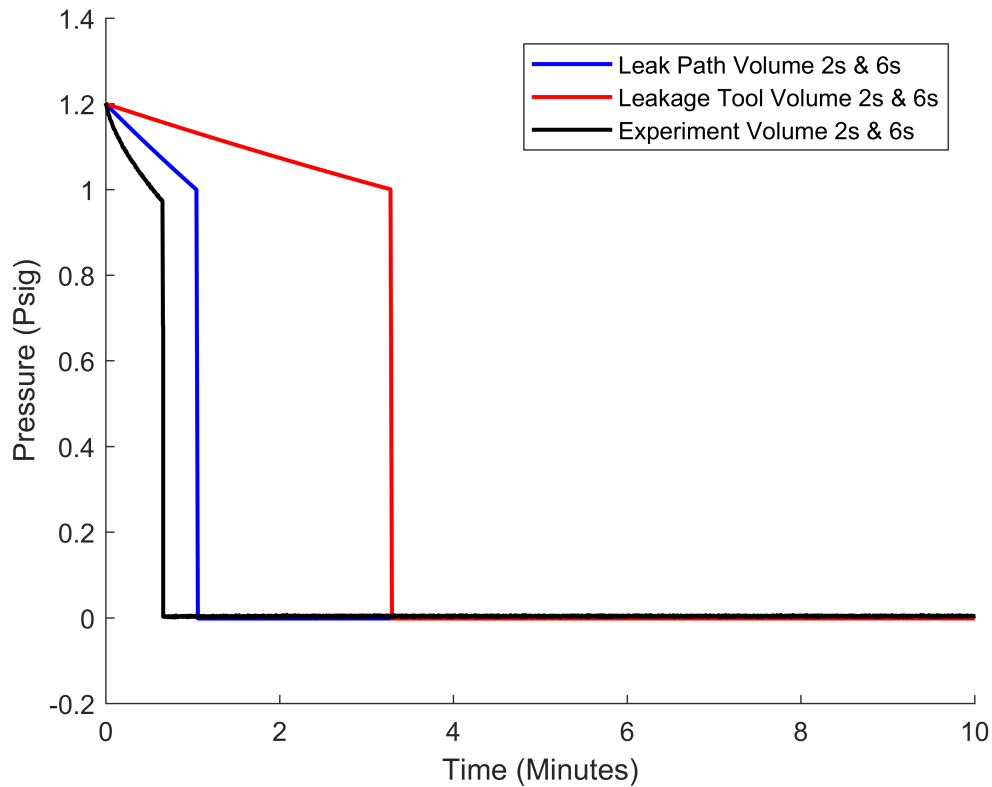


Figure 7.10: P2-C Pressure Response

Figure 7.11 shows the experimental data and GOTHIC simulations for the oxygen concentration in Volume 2s (CV3) and Volume 6s (CV6). Both experimental data and the GOTHIC simulations show that air refill occurs rapidly if the vent path is failed open. As it is depicted in Figure 7.11 leakage models used in simulations doesn't make difference in oxygen concentrations since the air flows predominantly through large-area RB vent path. Extrapolation of the curves indicate that both the experimental results and GOTHIC simulations would show air refill within about 60 minutes.

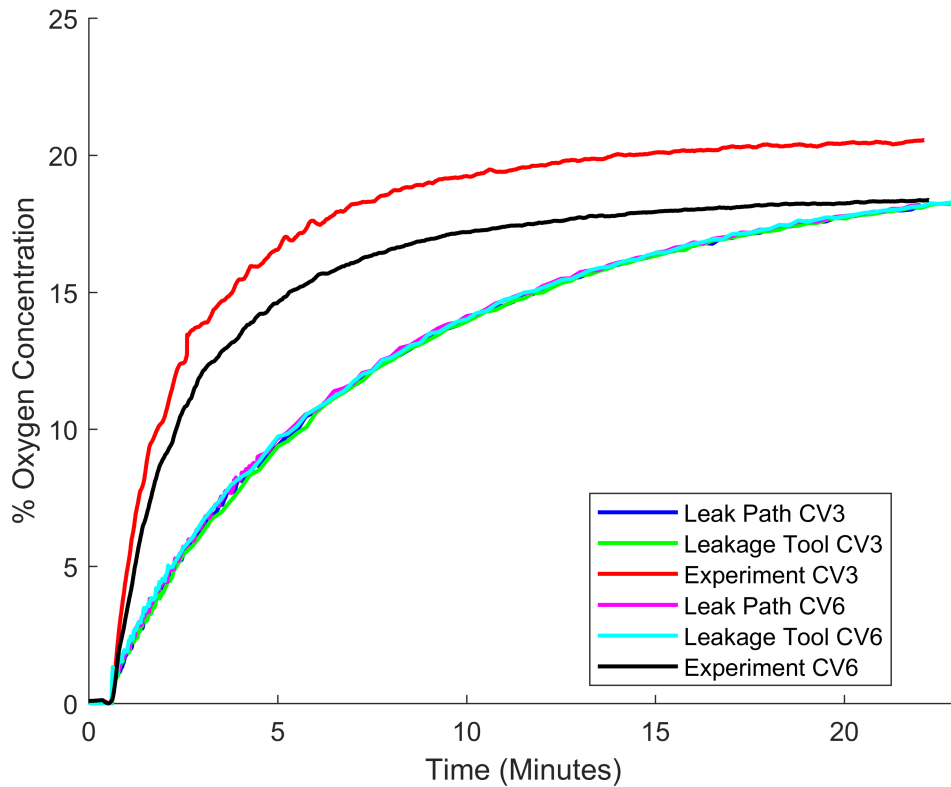


Figure 7.11: P2-C Oxygen Concentration Inside Facility

7.3 Phase III

Simulations for phase 3 are performed to characterize depressurization events of TAMU NGNP Test Facility, based on the tests P3A-1 and P3A-2. Since CV1 was isolated from the rest of the facility during these tests, CV1 is not modeled for these simulations. GOTHIC model consists only Volume 2s and Volume 6s connected through volumes 4s, 7s, 8s and Volume 9s. Doors (3D and 4D) were added to the model on both sides of Volume 4s to represent the aluminium plate and hinged louver respectively. Volume 5s is directly connected to Volume 3s (Atmosphere) with 3D connector 8 representing the flow path V5A. Flow boundary condition was included in the model to simulate the He injection at the top

of Volume 2s. Figure 7.12 shows the GOTHIC model nodalization for Phase 3 simulations.

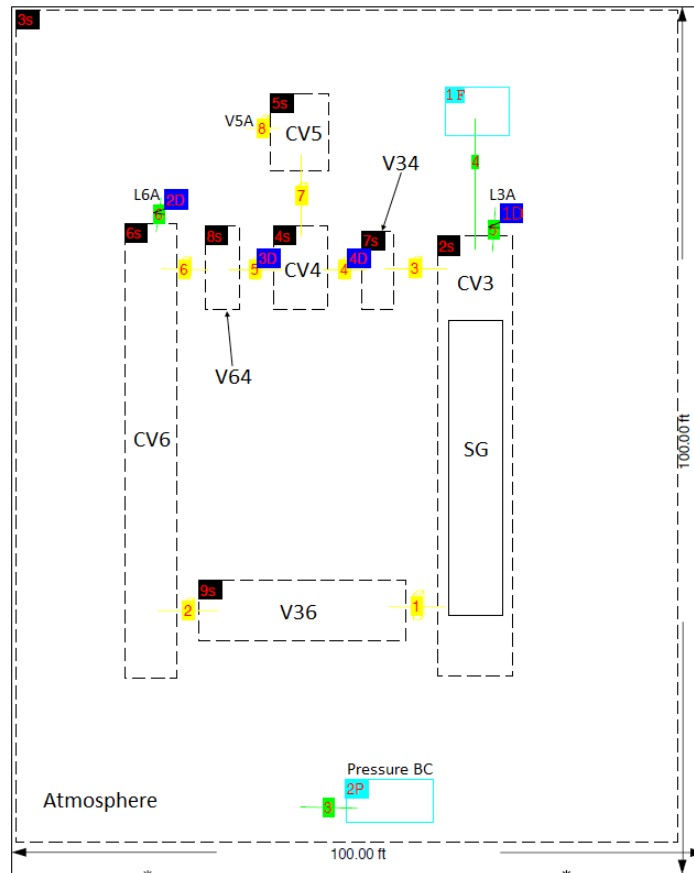


Figure 7.12: Phase 3 GOTHIC Model Nodalization

7.3.1 P3A-1

P3A-1 case is performed to simulate the RB compartments characteristic response during a hypothetical depressurization event. In P3A-1 test hinged louver was installed at V34, while the aluminium plate was installed at V64 (always closed). The hinged louver is simulated using an open trip options to door 4D. The door 4D is specified to be type "T OPEN", allowing for the door to open/close with a determined function. Leak path diameters for L3A and L6A are maintained as given in Table ???. P3A-1 simulation is isothermal.

A sensitivity analysis is performed to find the proper opening area fraction of 4D to match the experimental pressure response. Best results were obtained with door opening of 0.02% and closing for 99.99%.

7.3.1.1 Initial and Boundary Conditions

All boundary and initial conditions are set based on experimental setup. All compartments are initially filled with air. Flow boundary condition is set to mass flow rate of 1.68 kg/hr of helium. Temperature of injected helium and ambient air are set to 71.6 °F \approx 22°C. Trip to open the door 4D is set to 0.8 psig. Door 3D is always closed so that there is no flow on 3D connector number 5. Also, a trip is set to flow boundary condition to stop the flow of He at 430 seconds. P3A-1 is simulated for 450 seconds. Solution method is set to SEMI-IMPLICIT, pressure solution method is CONJUGATE and differencing scheme is BSOUP.

7.3.1.2 Results and Discussion

Figure 7.13 shows the GOTHIC simulations and experimental data for pressure response of RB. Pressure inside the volumes 2s and 6s increased until it reached the hinged louver operating pressure. Hinged louver in GOTHIC was modeled by placing door on 3D Connector 4 which connects volume 4s (CV4) to volume 7s (V34). Sensitivity analysis was made to the opening degree of hinged louver since it is unknown for the experiment. As it is depicted in Figure 7.13 following the hinged louver opening, pressure rapidly decreases and stays constant balancing the flow inertia with hinged louver resistance.

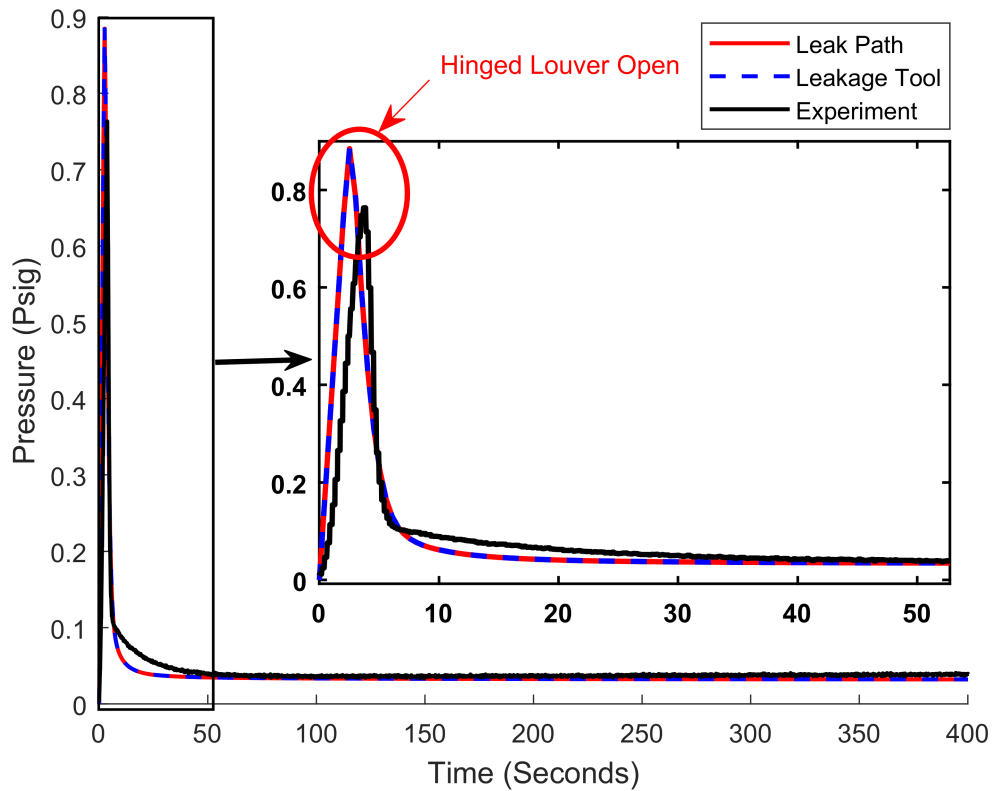


Figure 7.13: P3A-1 Pressure Response

As it can be seen in Figure 7.14 there is no change in oxygen concentration in experimental data and in GOTHIC simulations with both leakage models. Oxygen concentration in GOTHIC model remained at 21%. Figure 7.15 shows the three dimensional visualization of GOTHIC model for P3-A(1) depressurization scenario at 420 seconds. Figure 7.15 indicates that injected helium from the top of volume 2s was vented out through volume 4s and 5s to the atmosphere.

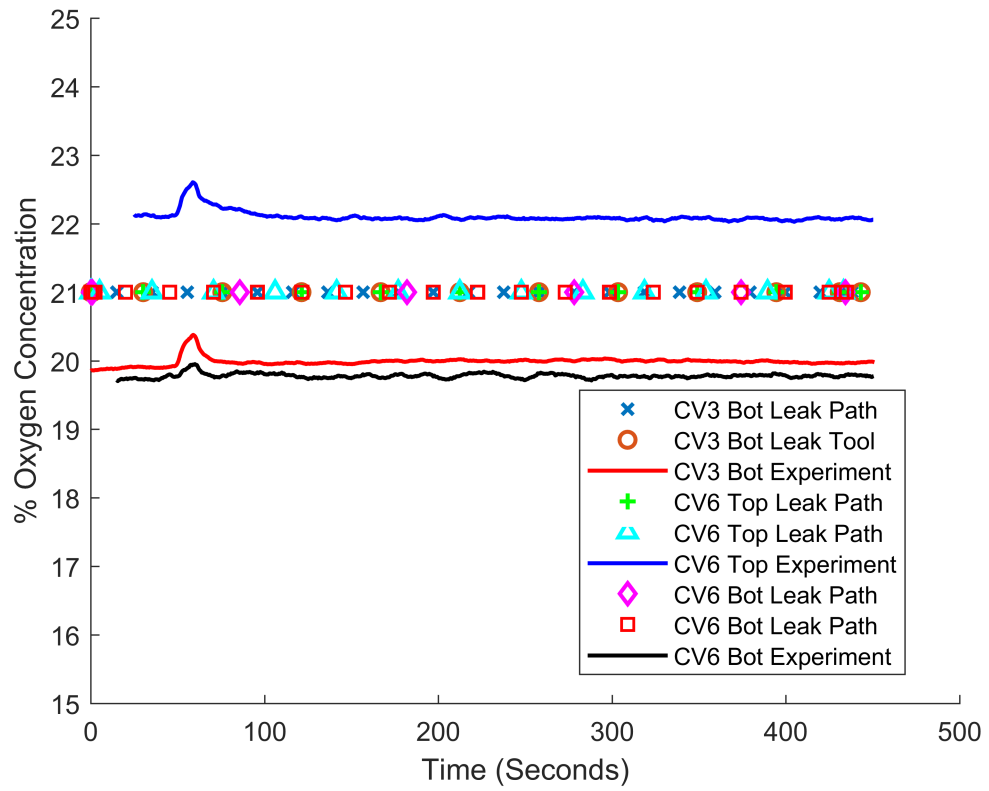


Figure 7.14: P3A-1 Oxygen Concentration

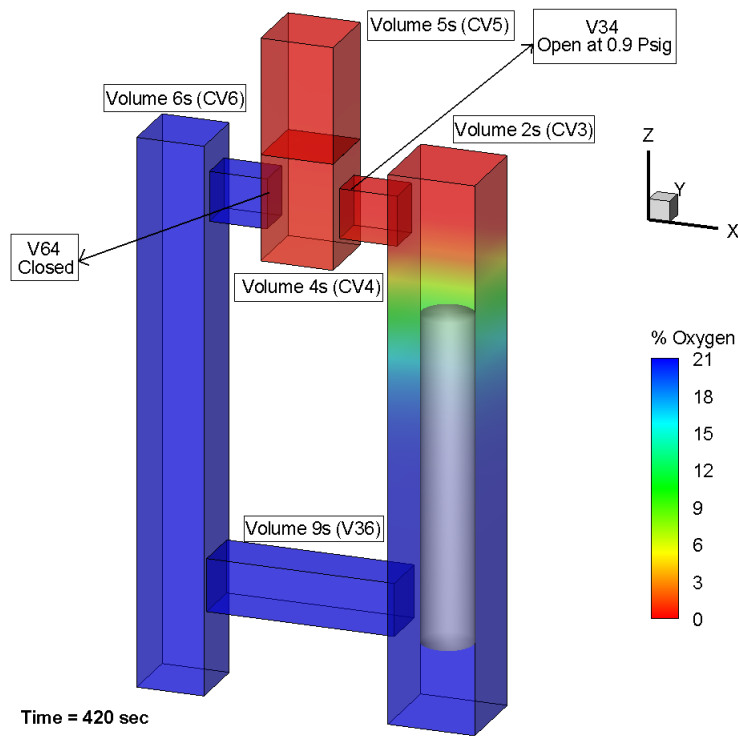


Figure 7.15: P3A-1 Oxygen Concentration at 420 Seconds

7.3.2 P3A-2

P3A-2 case is performed to simulate the RB compartments characteristic response during a hypothetical depressurization event and compare with experimental results. In P3A-2 test hinged louver is installed at V64 and the aluminium plate at V34. Simulation techniques are the same of the ones adopted for test P3A-1.

Similarly to what is done for test P3A-1, a sensitivity analysis on travel function is performed to best fit the pressure response and oxygen concentration with the experiment results. Best results are obtained with door opening of 0.02% and closing for 99.99% which are the same as in P3A-1.

7.3.2.1 *Initial and Boundary Conditions*

All cavities initially are filled with air. Flow boundary condition is set to mass flow rate of 1.68 kg/hr of helium. Temperature of injected helium and ambient air are set to 71.6 °F≈22°C. Trip to open the door 3D is set to 1.17 psig. Door 4D is always closed so that there is no flow on 3D connector number 4. Also, trip is set to flow boundary condition to stop the flow at 305 seconds. P3A-2 is simulated for 900 seconds. Solution method is set to SEMI-IMPLICIT, pressure solution method is CONJUGATE and differencing scheme is BSOUP.

7.3.2.2 *Results and Discussion*

For P3-A(2) case door on 3D Connector 4 is closed. Door on 3D connector 5 representing hinged louver opens when pressure inside the facility model reaches 1.2 psig. For this case, flow of injected helium from top of volume 2s is down through volume 2s and up through volume 6s before exiting RB as depicted in Figure 6.2. There is no specific data regarding to hinged louver opening range when the pressure inside the facility overcomes louver opening resistance. For this reason sensitivity analysis was made to the degree of opening by use of travel function in GOTHIC model. In the model it is assumed that hinged louver closes immediately following the helium flow shut off.

Figure 7.16 illustrates experimental pressure response data with GOTHIC model for both leakage models in facility for 500 seconds of simulation time. Hinged louver operation in simulation occurs at a slightly higher pressure. At around 320 seconds helium injection was terminated and it can be seen in experimental result clearly. However, in simulations after termination of helium injection pressure decays according to natural leak rate from the RB since the door representing the hinged louver was assumed to close immediately with helium shut off.

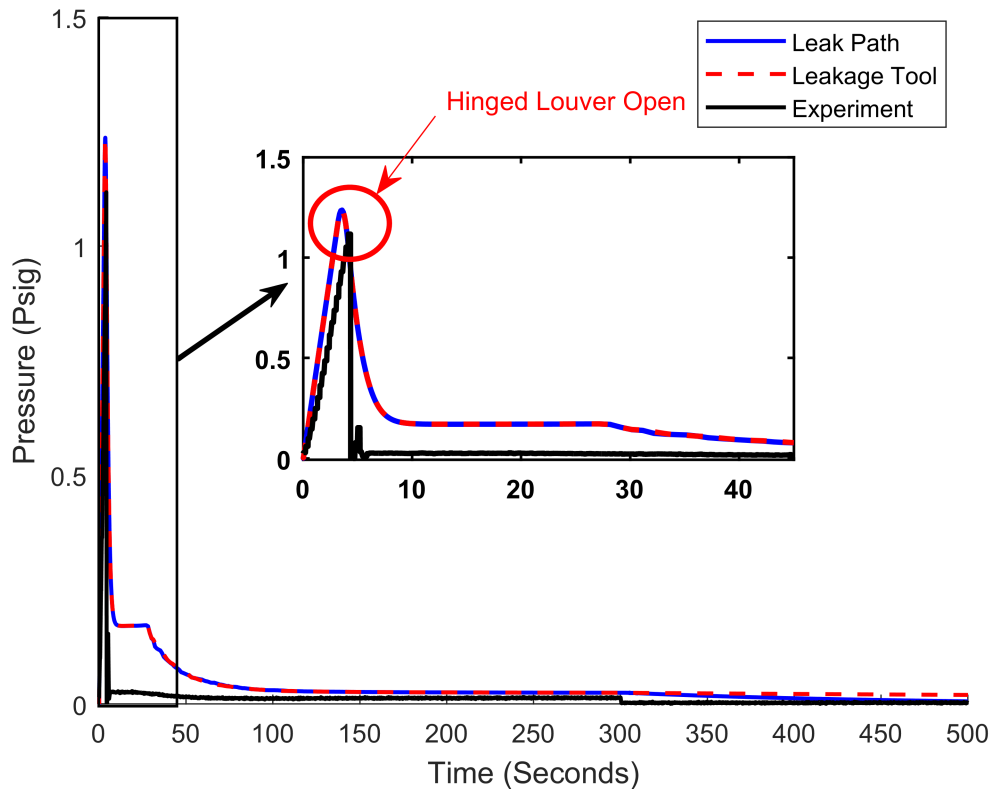


Figure 7.16: P3-A(2) Pressure Response

Figure 7.17 depicts the oxygen concentration inside the the test facility for experimental data and GOTHIC simulation results. Both the GOTHIC simulations and the experimental data show near complete flushing of air out of the bottom of volume 2s to the point when helium injection was terminated. The oxygen concentration then starts to slowly increase from air refill through the leak paths and the major contribution to the increase of oxygen concentration at the bottom of Volume 2s comes from the helium/air stratification due to buoyancy.

Because of the buoyancy oxygen concentration at the bottom of Volume 6s decreases slower than volume 2s bottom and volume 6s top. Injected helium from top of the Volume

2s pushes air to the volume 6s until pressure reaches to the hinged louver operating pressure. After that point helium flows to volume 6s through volume 9s and because of the buoyancy it tends to go up in volume 6s and trap the air at the bottom.

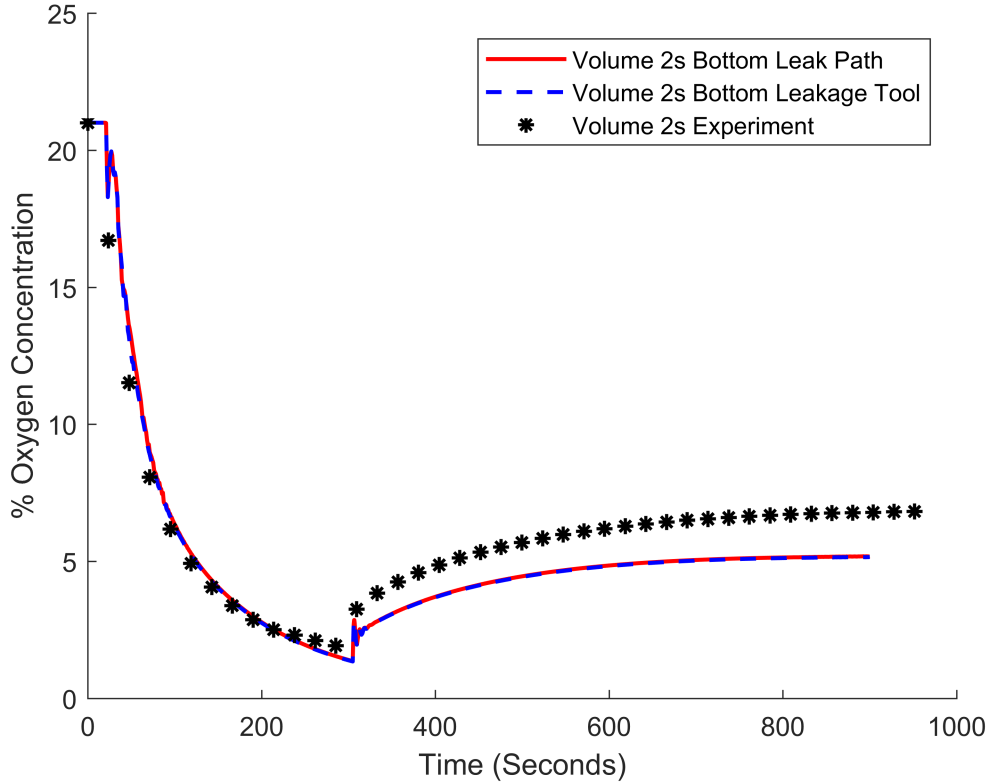


Figure 7.17: P3-A(2) Volume 2s Bottom Oxygen Concentration

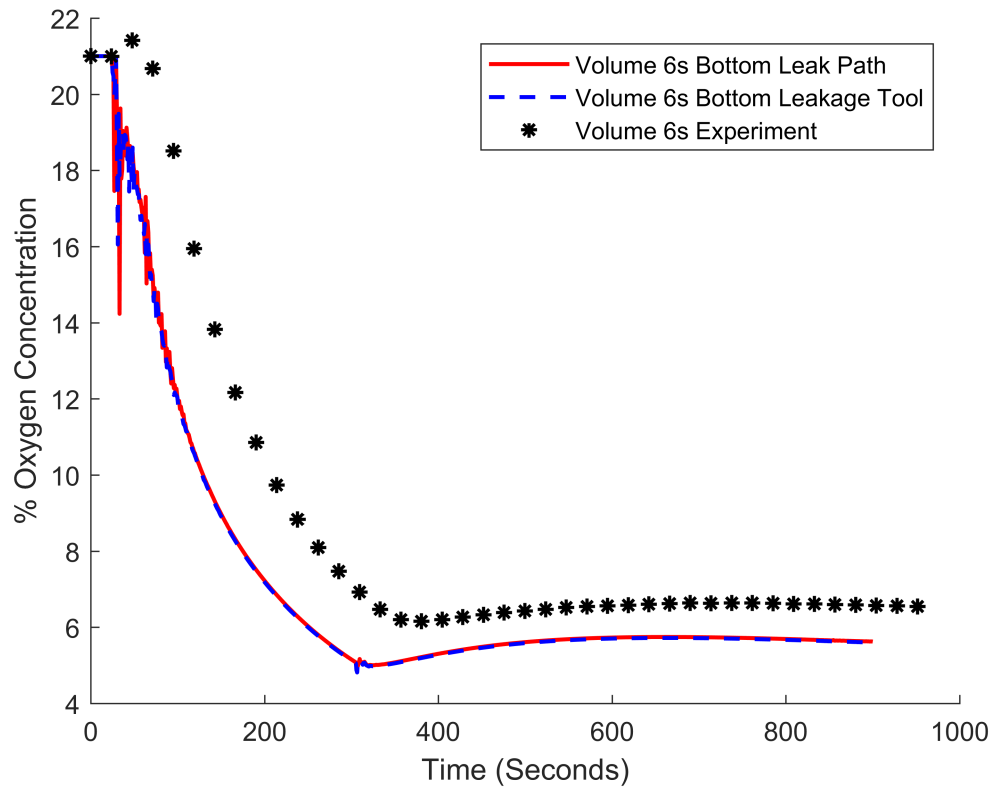


Figure 7.18: P3-A(2) Volume 2s Bottom Oxygen Concentration

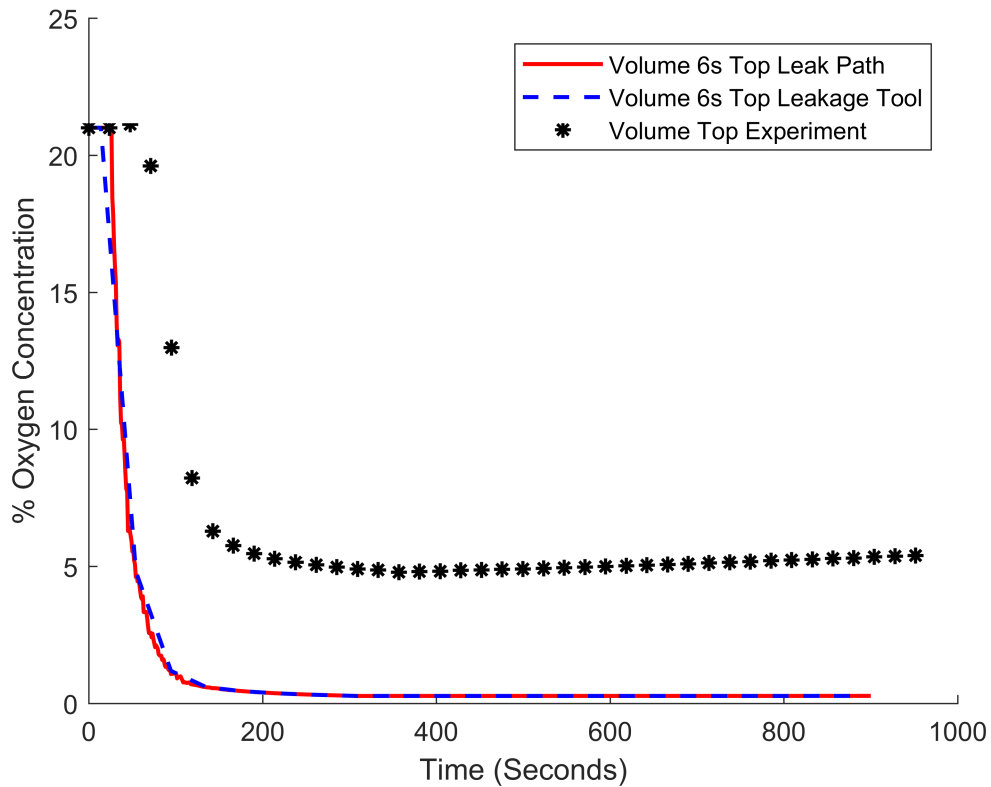


Figure 7.19: P3-A(2) Volume 2s Bottom Oxygen Concentration

Oxygen concentration on top of volume 6s decreases sharply to around 0% in GOTHIC simulations where it stays at around 5% in experiments. This shows that in experiments air is entering to CV6 while helium goes out which leads to 5% of air on top of CV6. However, helium flowing out dominates in simulations and there is no significant air entrance through hinged louver into volume 6s during the helium injection to volume 2s.

8. CONCLUSIONS

Three dimensional model of the simplified 1/28-scale HTGR reactor building test facility was developed with GOTHIC to perform simulations of depressurization scenarios of NGNP HTGR VLPC. Simulation results have been compared with the experimental data with the scope to validate the computer code performances and the ability to predict the behaviour during such scenarios.

Simulation results showed that the way of modeling the leakage from the volumes has a crucial effect on the results. Two methods were employed to simulate the natural leak rate of experimental facility with GOTHIC model. First method was to adding the leak paths to major volumes which simulates the total leakage from the compartment through single flow path and connects compartments with atmosphere and the second method is by using leakage model provided by GOTHIC code itself. Both models were able to replicate the test facility leak rates to simulate the response of a VLPC for depressurization scenarios. Further simulations for depressurization scenarios were performed with both leakage methods and results from each method were compared with experimental data.

Post-depressurization refill of air into the RB with vent paths working properly (P2-A case) was simulated with both leakage methods. The GOTHIC results were in satisfactory agreement with the experimental data for pressure in air refill simulations using the leakage tool provided by the code. Leak paths on top of the volumes resulted in much faster depressurization of volumes compared with the experiments. However, leak path method showed air refill into the RB compartment through leak paths if the RB vent path works as designed where the leakage model didn't show any air inside the volume. The experimental results may reflect incomplete flushing of air from the test facility prior to the test. Also it should be accounted for the uncertainties/limitations associated with the test

facility oxygen sensors as it can be seen from Figure 7.14 all three probes read different oxygen concentrations for fully air flushed compartments.

Simulations for the post-depressurization air refill into the RB where vent paths fail open showed air refill into the RB occurs rapidly as expected. It was also shown that leakage method doesn't affect oxygen concentration buildup in the facility when the large-area louver is open and flow is predominantly through the louver.

The GOTHIC simulations were in good agreement with the experimental data for the depressurization scenarios. In P3-A(1) case, GOTHIC simulations of test facility and experimental results show the reference vent path is effective at relieving pressure but is not effective at flushing air out of the steam generator cavity and equipment shaft for a break occurring near the top of the steam generator. Helium tends to go through short path since the break is near the reference vent path. The P3-A(2) simulation results and experimental data show that alternative vent path is very effective in venting out the air from the SG and equipment shaft cavities. Natural leakage from the cavities doesn't play any major role in pressure response or oxygen concentration in RB for both scenarios since the flow is predominantly from vent paths.

The results of this study have satisfactory agreement with experimental data. However, it should be noted that the way how leakage modeled from the compartments in this study are much more complex in reality. It accounts in reality for glued faces on the CVs, all fittings screwed on the faces of the compartments and in experiments there were two needle valves used to adjust the leakage from the compartments instead of single leak path as in simulations.

For the future work, CFD simulations could be performed for the higher accuracy in oxygen concentrations and better understanding of Loss of Forced Cooling (LOFC) accident scenarios.

9. FUTURE WORK

Many different methods and analysis have been left to future due to scope of this work. There are some ideas that I would like to try in this study which also can be worked in the future. The ideas that could be tested are as follows:

1. Leakage could be modeled more complex which would account for more details of the RB compartments. Leakage model could be used together with leak paths or multiple leak paths from the single volume can be used to model the leakage.
2. Turbulence models of the GOTHIC code could be added to the model to analyze the effect of turbulence to the gas concentration.
3. Computational Fluid Dynamics (CFD) tools could be used to analyze the local phenomena and for more precision and accuracy.

REFERENCES

- [1] “AREVA HTGR high temperature gas-cooled reactor information kit,” March 2005.
- [2] S. Yang, M. Silberberg, C. Fullerton, T. Nguyen, R. Vaghetto, and Y. Hassan, “Experimental study on a simplified facility of HTGR reactor building response to depressurization accidental scenarios,” (Las Vegas), 2016.
- [3] S. R. Yang, E. Kappes, T. Nguyen, R. Vaghetto, and Y. Hassan, “Experimental study on 1/28 scaled NGNP HTGR reactor building test facility response to depressurization event,” *Annals of Nuclear Energy*. Accepted December 2017.
- [4] 109th Congress, “Energy Policy Act of 2005.”
- [5] J. M. Beck and L. F. Pincock, “High temperature gas-cooled reactors lessons learned applicable to the next generation nuclear plant,” , Idaho National Laboratory, April 2011.
- [6] Generation IV International Forum, “Very high temperature reactor (VHTR).” https://www.gen-4.org/gif/jcms/c_9362/vhtr. Online; accessed 26 June 2017.
- [7] M. Richards, A. Baxter, C. Ellis, O. Gutierrez, and J. Crozier, “Conceptual design of the NGNP reactor system,” (Anaheim, California, USA), 2012.
- [8] L. Loflin, “Containment versus confinement for high-temperature gas reactors,” , EPRI, May 2005.
- [9] H. Haque, “Consequences of delayed air ingress following a depressurization accident in a high temperature reactor,” *Nuclear Engineering and Design*, vol. 238, no. 11, pp. 3041–3046, 2008.
- [10] C. Zhipeng, C. Xiaoming, Z. Yanhua, S. Jun, C. Fubing, S. Lei, L. Fu, D. Yujie, and Z. Zuoyi, “Air ingress analysis of chimney effect in the 200 MWe pebble-bed

- modular high temperature gas-cooled reactor,” *Annals of Nuclear Energy*, vol. 106, pp. 143–153, 2017.
- [11] GA TECHNOLOGIES INC., “Probabilistic risk assessment for the standard modular high temperature gas-cooled reactor,” 1987.
- [12] Numerical Applications Inc., *GOTHIC 8.1 Thermal Hydraulic Analysis Package User’s Manual*, 2014.
- [13] M. B. Silberberg, “Design and preliminary measurements inside of a simplified high temperature gas-cooled reactor building,” Master of Science Thesis, Texas A&M University, College Station, TX, 2017.
- [14] E. Kappes, S. Yang, R. Vaghetto, and Y. Hassan, “Experimental investigation of depressurization characteristics on the 1/28 scaled simplified HTGR reactor building model,” (Xi’an, Shaanxi, China), 17th International Topical Meeting on Nuclear Reactor Thermal Hydraulics, 2017.